NBER WORKING PAPER SERIES

ARE WE FRAGMENTED YET?
MEASURING GEOPOLITICAL FRAGMENTATION AND ITS CAUSAL EFFECT

Jesús Fernández-Villaverde
Tomohide Mineyama
Dongho Song

Working Paper 32638
http://www.nber.org/papers/w32638

NATIONAL BUREAU OF ECONOMIC RESEARCH
1050 Massachusetts Avenue
Cambridge, MA 02138
June 2024

We thank Torben Andersen, Philip Barrett, Christiane Baumeister, Dario Caldara, Steven Davis, Banu Demir, Xavier Gabaix, Lukas Hack, James Hamilton, Anna Ilyina, Benjamin Kett, Markus Pelger, Andrea Presbitero, Michele Ruta, Allan Timmermann, Mark Watson, Jonathan Wright and participants at numerous conferences and seminars for their comments and suggestions. The views expressed herein are those of the authors and should not be attributed to the IMF, its Executive Board, its management, or the National Bureau of Economic Research.

Are We Fragmented Yet? Measuring Geopolitical Fragmentation and Its Causal Effect
Jesús Fernández-Villaverde, Tomohide Mineyama, and Dongho Song
NBER Working Paper No. 32638
June 2024
JEL No. C11, C31, E00, F01, F2, F4, F6

ABSTRACT

After decades of rising global economic integration, the world economy is fragmenting. To measure this, we introduce a geopolitical fragmentation index based on a dynamic hierarchical factor model with time-varying parameters and stochastic volatility. We then use structural vector autoregressions and local projections to assess the causal effects of fragmentation. Increased fragmentation negatively impacts the global economy, with emerging economies suffering more than advanced ones. Notably, fragmentation has an immediate negative effect, while the benefits of reduced fragmentation unfold gradually. A sectoral analysis shows that industries closely tied to global markets are more adversely affected. Finally, we highlight significant differences in the effects of fragmentation across geopolitical blocs.

Jesús Fernández-Villaverde
Department of Economics
University of Pennsylvania
The Ronald O. Perelman Center
for Political Science and Economics
133 South 36th Street Suite 150
Philadelphia, PA 19104
and CEPR
and also NBER
jesusfv@econ.upenn.edu

Tomohide Mineyama
International Monetary Fund
700 19th Street, N.W.
Washington, DC 20431
tmineyama@imf.org

Dongho Song
Johns Hopkins University
Carey Business School
100 International Drive
Baltimore, MD 21202
dongho.song@jhu.edu

1 Introduction

After decades of increasing global economic integration, the world economy shifted course following the 2007-2008 financial crisis. Events such as Brexit, the invasion of Ukraine, and conflicts in the Middle East have strained international relations, prompting policymakers to rethink economic strategies. Free trade agreements, once common, have become rare, and trade-restricting measures in 2022 nearly tripled compared to 2019. As a result, households, firms, and governments are reassessing their operations amid rising geopolitical and trade complexities. For more on geopolitical fragmentation and its economic impact, see Aiyar et al. (2023a) and Gopinath (2023).

Yet, the definition and measurement of geopolitical fragmentation remain unclear. Is it primarily trade-related, marked by declining overall trade flows? Or does it reflect a shift toward intra-bloc trade, reducing cross-bloc interaction? While aggregate trade flows may seem stable, rising trade restrictions, policy uncertainty, and tariffs signal deeper fragmentation.

Moreover, fragmentation extends beyond trade. Financial fragmentation can emerge through capital market decoupling or alternative payment systems. Mobility fragmentation appears in stricter immigration policies and reduced international collaboration. Political realignments—driven by wars, energy disputes, and geopolitical tensions—often amplify these trends, creating feedback loops across domains.

In other words, geopolitical fragmentation is inherently multifaceted and challenging to define, let alone measure. Thus, choosing one indicator of fragmentation over another (or an average of them) to study its evolution and implications can be arbitrary and may lead to incorrect conclusions or policy recommendations.

To address this challenge, we develop a framework using a dynamic hierarchical factor model that treats geopolitical fragmentation as an unobservable set of variables. By combining widely used empirical indicators as noisy proxies, the model captures both the specific forces driving fragmentation—across trade, finance, mobility, and politics—and the overarching trends shared across these domains, giving us an operational measure of fragmentation. This approach moves beyond the simplistic view of fragmentation as the opposite of globalization, allowing us to gauge its interconnected processes in a way that resonates with policymakers, practitioners, and academics alike.

More concretely, we build on the tradition of dynamic factor models (DFMs), which provide a numerical measure of this multifaceted process. The core idea, pioneered by Sargent and Sims (1977), Geweke (1977), and Stock and Watson (1989), is that multiple observed indicators of a phenomenon—such as the business cycle or, in our case, geopolitical fragmentation—are driven by one or more common unobserved factors. While each indicator is imperfect and subject to idiosyncratic noise, a likelihood-based approach allows us to estimate the unobserved index that captures the underlying dynamics of interest.

The DFM approach has gained popularity because it is data-driven and minimizes the subjective decisions a researcher needs to make. Specifically, we propose a state-of-the-art dynamic hierarchical factor model with time-varying parameters and stochastic volatility. Our flexible specification can accommodate missing observations and handle data with different frequencies.

There are two main reasons for estimating such a model. First, it allows us to gauge the evolution of geopolitical fragmentation. An increase in the common fragmentation factor indicates that the world economy is becoming more fragmented, thus providing a quantitative confirmation (or refutation) of more casual assessments and mitigating the possible confirmatory bias present in many qualitative evaluations by experts. Second, the estimated common fragmentation factor can be used as an input for other empirical analyses, such as a variable in a structural vector autoregression (SVAR) or a linear projection (LP) for causality assessment. This enables us to translate changes in the factor (e.g., an increase by one standard deviation) into concrete effects on aggregate variables with a sharp economic interpretation (e.g., a 0.4% reduction in GDP).

After introducing the indicators we employ and discussing our methodology, we present the evolution of our estimated common fragmentation factor. This index reveals three distinct phases. First, there was a period of relative stability in geopolitical fragmentation from 1975 to the early 1990s. Fragmentation then decreased as the collapse of the Soviet Union and market-oriented reforms across many countries led to a spike in globalization. However, following the 2007-2008 financial crisis, geopolitical fragmentation has increased to its highest levels in the sample, with no signs of reversal. Our estimation results align broadly with narrative approaches that have discussed the evolution of geopolitical fragmentation based on narrative evidence (e.g., Gopinath, 2023).

We also report estimated group-specific fragmentation factors. Our key finding is that, while substantial comovement exists across groups, group-specific fragmentation dynamics show notable heterogeneity. For instance, trade fragmentation declines more slowly than the common factor, falling below zero only around 2005, whereas the common factor began its decline around 1995. Moreover, trade fragmentation did not accelerate significantly post-2008 but has risen over the past eight years. Our results highlight that focusing only on trade fragmentation might be misleading. In contrast, financial fragmentation shows very strong comovement with the common factor.

We thoroughly validate the robustness of our fragmentation factors. For instance, we compare our estimated common fragmentation factor with those from a non-hierarchical DFM and a principal components analysis (PCA). Both approaches effectively capture common fragmentation dynamics, with PCA offering a simpler framework. However, PCA is less suited for handling missing observations and varying data frequencies, and neither framework accounts for hierarchical structure. This limitation underscores the added value of our

hierarchical DFM.

Next, we examine the world economy's fragmentation into distinct geopolitical blocs. We find notable differences in fragmentation levels between blocs, such as the U.S.-EU bloc vs. the China-Russia bloc. Fragmentation shocks in the U.S.-EU bloc have more pronounced global effects than those in the China-Russia bloc, underscoring the unique nature of the latter economic relationship.

Finally, we use our common fragmentation factor as an input for causality analysis with SVARs and LPs. A one-standard-deviation shock to the fragmentation factor (an adverse event) negatively impacts the global economy, with stronger effects on emerging economies than advanced ones. The impacts are asymmetric: fragmentation has an immediate negative effect, whereas the benefits of reduced fragmentation (a facet of globalization) emerge with lags. Our findings remain robust under different identification assumptions (e.g., variable orderings or a narrative approach) and with various control variables, as in Caldara and Iacoviello (2022).

To clarify the economic channels through which fragmentation affects the economy, we analyze sectors within OECD economies. The sectoral analysis reveals adverse effects on industries closely tied to global markets, such as manufacturing, construction, finance, and wholesale and retail trade. In contrast, sectors like agriculture, forestry, fishing, real estate, and public services, which are more insulated, experience only marginal effects.

Our paper contributes to the expanding literature on geopolitical fragmentation (e.g., Attinasi et al., 2023, Blanga-Gubbay and Rubinova, 2023, Bolhuis et al., 2023, Campos et al., 2023, Cerdeiro et al., 2021, Clayton et al., 2024, Góes and Bekkers, 2022, Hakobyan et al., 2023, Javorcik et al., 2024, and Utar et al., 2023), building on the summaries provided by Aiyar et al. (2023a) and Gopinath (2023). This literature sheds light on the associated costs, which include the unwinding of gains from globalization, encompassing trade (e.g., Frankel and Romer, 1999; Feenstra, 2006; technology diffusion and adoption (e.g., Bartelme and Gorodnichenko, 2015; Bustos, 2011; Acemoglu et al., 2015), cross-border labor and capital flows (e.g., Glennon, 2024; Erten et al., 2021), and international risk sharing (e.g., Obstfeld, 1994). Our paper adds to this body of work by quantifying the causal effects of fragmentation on aggregate economic variables. While existing papers focus on a single or a few indicators of fragmentation (e.g., Antràs, 2020, Goldberg and Reed, 2023, and Gopinath et al., 2025), our approach aggregates a wide range of measures of fragmentation.

Geopolitical tensions contribute to increased uncertainty regarding future policies and the ultimate shape of a fragmented world (e.g., Caldara et al., 2020). The direct costs of trade disruptions include tariffs, inefficiencies from reduced specialization, resource misallocation, diminished economies of scale, and decreased competition (e.g., Melitz and Trefler, 2012). Aiyar et al. (2023a) point out that short-term transition costs stemming from trade disruptions tend to be more pronounced due to the low elasticities of substitution in the short run.

In contrast, losses from technological decoupling may materialize over the medium and long term. Our empirical findings point out the importance of those longer-horizon considerations.

Moreover, our empirical results confirm the previous findings that the impact of these costs may vary across countries. As highlighted by Aiyar et al. (2023a), geoeconomic fragmentation disproportionately affects emerging markets and low-income countries that have the potential for catch-up through trade and financial and technological integration. Gopinath (2023) and Gopinath et al. (2025) add that if disruptions occur primarily between large blocs (e.g., a U.S.-Europe bloc and a China-Russia bloc), some countries, particularly in Latin America or Southeast Asia, may experience gains as "neutral" bystanders.

Given the multiple channels of impact and potential heterogeneity described above, the examination of the cost of fragmentation is an empirical question. The literature has investigated the economic consequences of recent fragmentation episodes, such as Brexit (e.g., Sampson, 2017, and Bloom et al., 2019) and the U.S.-China trade war in 2018-19 (e.g., Flaaen and Pierce, 2019; Fajgelbaum and Khandelwal, 2022; Fajgelbaum et al., 2019). A few studies (Góes and Bekkers, 2022, Cerdeiro et al., 2021, and Bolhuis et al., 2023) develop general equilibrium international trade models to estimate the cost of fragmentation. Our SVAR and LP estimates add new findings to these previous results.

Finally, our paper contributes to the existing body of literature focused on formulating indices or metrics. This includes assessments of uncertainty (e.g., Jurado et al., 2015, and Baker et al., 2016), geopolitical risks (e.g., Caldara and Iacoviello, 2022), economic state evaluations (e.g., Aruoba et al., 2009, and Shapiro et al., 2022), investor sentiment analysis (e.g., Baker and Wurgler, 2007), corporate credit market scrutiny (e.g., Gilchrist and Zakrajšek, 2012), shadow rate investigations (e.g., Wu and Xia, 2016), and considerations of measures related to the COVID-19 pandemic as presented by Arias et al. (2023), along with disruptions in the supply chain discussed by Bai et al. (2024).

The paper is organized as follows. Section 2 examines the empirical indicators of geopolitical fragmentation. Section 3 introduces a dynamic hierarchical factor model and constructs the geopolitical fragmentation index. Section 4 evaluates its causal impact on economic aggregates. Section 5 concludes. The Appendix includes additional details and robustness exercises.

2 Empirical Indicators of Geopolitical Fragmentation

The 16 indicators we compile capture different dimensions of geopolitical fragmentation, each reflecting disruptions in trade, finance, mobility, or political alignments. We first list their sources and classify them into four groups—trade, financial, mobility, and political—to highlight the varied forms of fragmentation.

2.1 Data sources for geopolitical fragmentation indicators

We begin by listing each indicator and its sources:

1. The trade openness ratio, (export+import)/GDP, from the International Financial Statistics (IFS).
2. The number of trade restrictions, from the Global Trade Alert.
3. The temporary trade barriers, from Bown et al. (2020).
4. The trade policy uncertainty, from Caldara et al. (2020).
5. The tariff, from Alesina et al. (2020).
6. The FDI ratio, calculated as FDI/GDP, from the IFS.
7. The financial flow ratio, (portfolio investment+other investment)/GDP, from the IFS.
8. The capital control measure, from Fernández et al. (2016).
9. The migration flow ratio, net migration flows as a percentage of the population, from UN World Population Prospects.
10. The patent flows, from International Patent and Citations across Sectors (INPACT-S) compiled by LaBelle et al. (2023).
11. The migration fear index, from Bloom et al. (2015).
12. The geopolitical risk index, from Caldara and Iacoviello (2022).
13. The energy uncertainty, from Dang et al. (2023).
14. The number of conflicts, based on the Uppsala Conflict Data Program.
15. The number of sanctions, from Felbermayr et al. (2020).
16. The UN General Assembly kappa score, from Häge (2017).

The detailed descriptions of the indicators are in Appendix A.1. Panel (A) of Figure 1 plots their time series. In the trade domain, measures like trade openness have stagnated since the 2007-2008 financial crisis. Financial indicators, including the financial flow ratio, show a similar decline in global integration. Political indicators, such as the number of sanctions, trend upward, signaling increased fragmentation. In mobility, a spike in migration-related fear highlights rising concerns about cross-border movement. Panel (B) provides summary statistics, including non-stationarity tests and pairwise correlations with trade openness (using

Figure 1: Indicators for fragmentation

(A) Time series

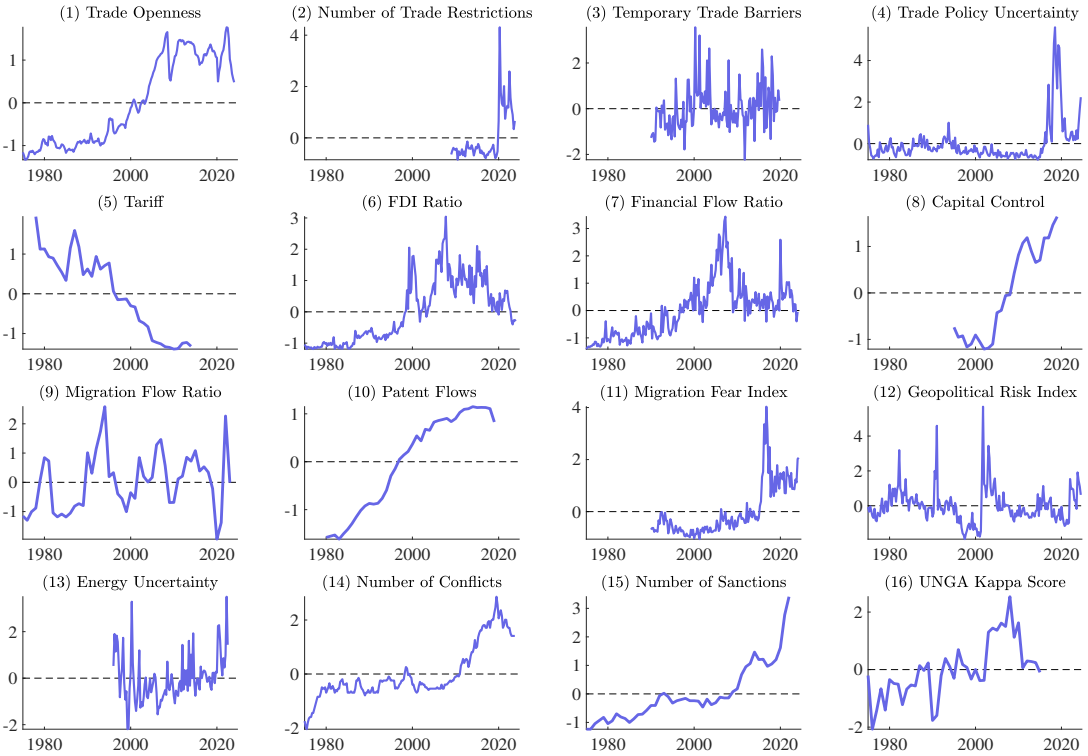

(B) Summary statistics

Category	Individual Indicators	Sample	Freq.	ADF test (p-value)	Correlation w/ Trade Openness
Trade fragmentation	Trade Openness	1975-2024	Q	0.17	1.00
	Number of Trade Restrictions	2009-2023	Q	0.09	-0.06
	Temporary Trade Barriers	1990-2019	Q	0.00	0.27
	Trade Policy Uncertainty	1975-2024	Q	0.02	0.24
	Tariff	1978-2014	A	0.11	-0.92
Financial fragmentation	FDI Ratio	1975-2024	Q	0.07	0.85
	Financial Flow Ratio	1975-2024	Q	0.04	0.77
	Capital Control	1995-2019	A	0.71	0.83
Mobility fragmentation	Migration Flow Ratio	1975-2023	A	0.00	0.31
	Patent Flows	1980-2019	A	0.10	0.92
	Migration Fear Index	1990-2024	Q	0.13	0.49
Political fragmentation	Geopolitical Risk Index	1975-2024	Q	0.00	-0.11
	Energy Uncertainty	1996-2022	Q	0.00	0.07
	Number of Conflicts	1975-2023	Q	0.16	0.71
	Number of Sanctions	1975-2022	A	0.99	0.79
	UNGA Kappa Score	1975-2015	A	0.01	0.67

Notes: For comparability, all indicators are standardized to zero mean and unit standard deviation. Except for those from text mining, indicators represent the average across countries with available data. We report the p-value from the augmented Dickey-Fuller test, where the null hypothesis assumes non-stationarity.

annual aggregated data). Our dynamic hierarchical factor model is motivated by the observation that, while indicators show comovement, substantial idiosyncratic behavior remains, underscoring the need for a framework that captures both global trends and group-specific variations.

2.2 Categorizing indicators into four key fragmentation groups

Next, we review the literature on the relevance of our 16 indicators of geopolitical fragmentation, along with potential caveats. These indicators fall into four categories: (i) trade, (ii) financial, (iii) mobility, and (iv) political fragmentation.

Trade fragmentation

Globalization has been driven by the free flow of goods and services across borders, with trade openness serving as a key indicator of its progress (*indicator 1*). Aiyar et al. (2023b) and Gopinath (2023) observed that while trade expanded significantly during the hyperglobalization phase of the 1980s, it has stagnated since 2008—a phenomenon known as "slowbalization." Gopinath (2023) noted that trade-to-GDP ratios have stabilized, reflecting the natural waning of the forces that once propelled hyperglobalization.

Trade dynamics are also shaped by measures that restrict or facilitate flows. Non-tariff barriers, such as trade restrictions from the Global Trade Alert (*indicator 2*) and temporary trade barriers from Bown et al. (2020) (*indicator 3*), significantly influence global trade patterns.[1] Trade policy uncertainty (*indicator 4*), as described by Caldara et al. (2020), underscores risks from shifting trade dynamics. Tariffs (*indicator 5*) remain the primary policy tool affecting trade. Together, these indicators offer a broad view of trade dynamics and globalization.

While these measures help us understand fragmentation, their effects are difficult to quantify due to country-specific factors. For example, the trade share of developing countries might decline due to weak domestic demand and structural shifts, such as the growth of their non-tradable service sectors. Furthermore, economic cycles affect trade dynamics.

Financial fragmentation

Cross-border financial integration, a pillar of globalization, is measured through the FDI ratio (*indicator 6*) and financial flow ratio (*indicator 7*). Like trade, financial flows surged in the late 20th century but have stagnated or declined since 2008. A key driver of financial fragmentation is capital control measures (*indicator 8*), which regulate cross-border capital flows

[1] Measuring non-tariff barriers is hard. Trade restrictions and temporary trade barriers rely on similar but slightly different definitions, detailed in Appendix A.1, and vary in country coverage and period.

by shaping financial system openness. However, their effects require careful interpretation, as they may respond to economic shocks, complicating their role in financial integration.

Mobility fragmentation

Mobility fragmentation captures barriers to the movement of people and ideas, reflected in migration flows (*indicator 9*), patent flows (*indicator 10*), and the migration fear index (*indicator 11*), developed by Bloom et al. (2015) to assess public attitudes toward migration—insights often missing in traditional "hard" data. However, migration dynamics also depend on broader economic cycles and domestic factors, such as weak aggregate demand in developing countries and structural shifts in developed economies toward non-tradable sectors. We should consider these factors when interpreting the data.

Political fragmentation

Political fragmentation reflects geopolitical instability and misalignment, measured through various indices and datasets. The geopolitical risk index (*indicator 12*) captures events like wars and terrorism, while the energy uncertainty index (*indicator 13*) highlights tensions over energy supply. Violent conflicts, documented by the Uppsala Conflict Data Program (*indicator 14*), directly manifest political fragmentation. Economic sanctions (*indicator 15*), categorized by Felbermayr et al. (2020) into trade, financial, and military assistance, restrict cross-border flows and shape political dynamics. Not all tensions escalate into conflict; political alignment can also be gauged through subtler measures, such as UNGA voting behavior. Häge (2017) introduced the "kappa score" (*indicator 16*), which quantifies bilateral voting alignment, offering a nuanced view of political relationships. Together, these measures capture the multifaceted nature of political fragmentation.

However, interpreting political fragmentation in isolation is misleading. It interacts with and often drives fragmentation in trade, finance, and mobility while itself being shaped by economic forces. Though categorized separately, we should study these dimensions in tandem.

2.3 Discussion

How can we quantify comovements among diverse geopolitical fragmentation indicators and extract their shared information? A simple average is inadequate, as it ignores each indicator's varying importance, and imposing arbitrary weights is equally unjustified. Instead, we use a likelihood-based approach that let the data determine the appropriate weights, We discuss this estimation strategy next.

3 Measuring Geopolitical Fragmentation

In this section, we treat geopolitical fragmentation as an unobservable set of variables, with each indicator serving as a noisy proxy. This approach enables us to employ a likelihood-based framework, allowing each indicator dynamics to determine the optimal weights for estimating latent factors. The framework is flexible, accommodating additional indicators or replacements while remaining robust to the exclusion of subsets of the 16 selected indicators.

We employ a dynamic hierarchical factor model that identifies both commonalities and group-specific variations. The model leverages the natural categorization of indicators into four groups—trade, financial, mobility, and political—reflecting distinct fragmentation dimensions. This hierarchical structure accounts for shared dynamics driving overall fragmentation while allowing for idiosyncratic group-specific behavior.

Factor models have been central to economic analysis since the unobservable index models of Sargent and Sims (1977) and Geweke (1977). The pioneering work of Stock and Watson (1989) reinforced their role in extracting valuable information from macroeconomic time series for forecasting. Our model builds on Moench et al. (2013) and follows the foundations of Del Negro and Otrok (2008) and Del Negro and Schorfheide (2011), using Bayesian estimation techniques. This methodology traces back to Geweke and Zhou (1996) and Otrok and Whiteman (1998).

3.1 Specification

Let $k \in \{1, \ldots, N_j\}$ be the set of indices for the different indicators of geopolitical fragmentation classified in a group $j \in \{1, \ldots, J\}$. In our case, $\sum_j N_j = 16$, but it could be any other finite natural number, with the only limitation being computational capabilities. The value that each indicator within a group j takes at time t is then $y_{k,t}^{(j)}$.

We assume that the dynamics of $y_{k,t}^{(j)}$ are driven by a group-specific factor $f_t^{(j)}$:

$$y_{k,t}^{(j)} = a_{k,t}^{(j)} + b_{k,t}^{(j)} f_t^{(j)} + u_{k,t}^{(j)}, \tag{1}$$

which we interpret as the state of geopolitical fragmentation shared within a group j. In equation (1), the mean $a_{k,t}^{(j)}$, slope $b_{k,t}^{(j)}$, and error $u_{k,t}^{(j)}$ depend on both the indicator and time. In this way, we incorporate much flexibility in how the factor is linked with each indicator.

The group-specific factor itself is modeled as follows:

$$\begin{aligned} f_t^{(j)} &= \lambda^{(j)} f_t + \eta_t^{(j)}, \\ f_t &= f_{t-1} + \sigma_{f,t}\epsilon_{f,t}, \quad \epsilon_{f,t} \sim \mathcal{N}(0,1), \\ \eta_t^{(j)} &= \eta_{t-1}^{(j)} + \sigma_{f,t}^{(j)}\epsilon_{f,t}^{(j)}, \quad \epsilon_{f,t}^{(j)} \sim \mathcal{N}(0,1), \end{aligned}$$

where f_t is the common factor driving the comovement across J groups, and $\eta_t^{(j)}$ captures the group-specific dynamic component. Since both f_t and $\eta_t^{(j)}$ follow a random-walk process, the group-specific factor can be re-expressed as:

$$f_t^{(j)} = f_{t-1}^{(j)} + \lambda^{(j)}\sigma_{f,t}\epsilon_{f,t} + \sigma_{f,t}^{(j)}\epsilon_{f,t}^{(j)}, \quad \epsilon_{f,t} \sim \mathcal{N}(0,1), \quad \epsilon_{f,t}^{(j)} \sim \mathcal{N}(0,1).$$

When there are no group-specific shocks and all group-specific factors move proportionally, $\epsilon_{f,t}^{(j)} = 0$, reducing the model to a single-factor structure. In contrast, if each group-specific factor moves purely idiosyncratically, $\epsilon_{f,t} = 0$, and the model decomposes into J distinct group-specific factors.

To aid interpretation, an alternative specification to equation (1) is given by:

$$y_{k,t}^{(j)} = \underbrace{a_{k,t}^{(j)}}_{\substack{\text{idiosyncratic}\\ \text{deterministic}\\ \text{component}}} + \underbrace{b_{k,t}^{(j)}\lambda^{(j)} f_t}_{\substack{\text{common}\\ \text{factor}}} + \underbrace{b_{k,t}^{(j)}\eta_t^{(j)}}_{\substack{\text{group-specific}\\ \text{factor}}} + \underbrace{u_{k,t}^{(j)}}_{\substack{\text{idiosyncratic}\\ \text{stochastic}\\ \text{component}}}, \tag{2}$$

where we decompose the group-specific factor into the component that is common across J groups and the component specific to group j. This framework parallels the approach of Moench et al. (2013) by distinguishing between variations that are common within groups but distinct across groups, $\eta_t^{(j)}$, and those that are genuinely common across all groups, f_t.

We assume that $a_{k,t}^{(j)}$ and $b_{k,t}^{(j)}$ evolve as:

$$\begin{aligned}
a_{k,t}^{(j)} &= a_{k,0}^{(j)} + a_{k,1}^{(j)} t, \\
b_{k,t}^{(j)} &= b_{k,t-1}^{(j)} + \sigma_{b_k}^{(j)}\epsilon_{b_k,t}^{(j)}, \quad \epsilon_{b_k,t}^{(j)} \sim \mathcal{N}(0,1), \\
u_{k,t}^{(j)} &= \rho_{u_k,1}^{(j)} u_{k,t-1}^{(j)} + ... + \rho_{u_k,q}^{(j)} u_{k,t-q}^{(j)} + \sigma_{u_k,t}^{(j)}\epsilon_{u_k,t}^{(j)}, \quad \epsilon_{u_k,t}^{(j)} \sim \mathcal{N}(0,1).
\end{aligned}$$

First, we address non-stationarity in the proxies $y_{k,t}^{(j)}$ by incorporating a deterministic time trend $a_{k,t}^{(j)}$ orthogonal to the group-specific factor $f_t^{(j)}$. This distinction is important, as shown in Panel (B) of Figure 1, where some indicators display a deterministic time trend while others do not. Our approach assumes that the common dynamics across empirical indicators are driven by a non-deterministic time component, which is modeled as a random-walk process.

Second, we accommodate time-varying sensitivities $b_{k,t}^{(j)}$ of individual proxies with respect to the group-specific factor $f_t^{(j)}$ through a random-walk process, capturing potential slow-moving variations. This flexibility is crucial, as certain indicators may reveal more about geopolitical fragmentation than others, and their importance can change over time.

Third, we allow the individual error terms $u_{k,t}^{(j)}$ to exhibit serial correlation, capturing dynamics that do not comove and are idiosyncratic to each series. This approach involves relaxing the assumption that all dynamics arise solely from the factor. The rationale behind this adjustment is to prevent the factor estimates from becoming overly dependent on a subset

of empirical indicators that exhibit high persistence.

Finally, the innovation variances, $\sigma_{g,t}^{(j)}$, are time-varying:

$$\begin{aligned}
&\sigma_{g,t}^{(j)} = \sigma_g^{(j)} \exp(h_{g,t}^{(j)}), \\
&h_{g,t}^{(j)} = h_{g,t-1}^{(j)} + \sigma_{h_g}^{(j)} \epsilon_{h_g,t}^{(j)}, \quad \epsilon_{h_g,t}^{(j)} \sim \mathcal{N}(0,1), \quad g \in \left\{f, u_1, \ldots, u_{N_j}\right\}.
\end{aligned}$$

This specification also applies to $\sigma_{f,t}$, where the superscript (j) is omitted to denote the common factor f_t:

$$\sigma_{f,t} = \sigma_f \exp(h_{f,t}), \quad h_{f,t} = h_{f,t-1} + \sigma_{h_f} \epsilon_{h_f,t}, \quad \epsilon_{h_f,t} \sim \mathcal{N}(0,1).$$

This property applies to innovations in both the factors (common and group-specific) and the idiosyncratic error terms. Incorporating stochastic volatility is essential not only for modeling the data's non-Gaussian features but also for capturing outlier events in certain years, affecting both factors and idiosyncratic terms. This dynamic approach enables the model to adapt to shifting volatility patterns, providing a more robust representation of the underlying dynamics in the empirical indicators.

Compiling all the previous equations, we get the complete specification of our model:

$$\begin{aligned}
&y_{k,t}^{(j)} = a_{k,t}^{(j)} + b_{k,t}^{(j)} f_t^{(j)} + u_{k,t}^{(j)}, \\
&a_{k,t}^{(j)} = a_{k,0}^{(j)} + a_{k,1}^{(j)} t, \\
&b_{k,t}^{(j)} = b_{k,t-1}^{(j)} + \sigma_{b_k}^{(j)} \epsilon_{b_k,t}^{(j)}, \quad \epsilon_{b_k,t}^{(j)} \sim \mathcal{N}(0,1), \\
&f_t^{(j)} = f_{t-1}^{(j)} + \lambda^{(j)} \sigma_{f,t} \epsilon_{f,t} + \sigma_{f,t}^{(j)} \epsilon_{f,t}^{(j)}, \quad \epsilon_{f,t} \sim \mathcal{N}(0,1), \quad \epsilon_{f,t}^{(j)} \sim \mathcal{N}(0,1), \\
&u_{k,t}^{(j)} = \rho_{u_k,1}^{(j)} u_{k,t-1}^{(j)} + \ldots + \rho_{u_k,q}^{(j)} u_{k,t-q}^{(j)} + \sigma_{u_k,t}^{(j)} \epsilon_{u_k,t}^{(j)}, \quad \epsilon_{u_k,t}^{(j)} \sim \mathcal{N}(0,1), \\
&\sigma_{g,t}^{(j)} = \sigma_g^{(j)} \exp(h_{g,t}^{(j)}), \quad h_{g,t}^{(j)} = h_{g,t-1}^{(j)} + \sigma_{h_g}^{(j)} \epsilon_{h_g,t}^{(j)}, \quad \epsilon_{h_g,t}^{(j)} \sim \mathcal{N}(0,1), \quad g \in \left\{f, u_1, \ldots, u_{N_j}\right\}, \\
&\sigma_{f,t} = \sigma_f \exp(h_{f,t}), \quad h_{f,t} = h_{f,t-1} + \sigma_{h_f} \epsilon_{h_f,t}, \quad \epsilon_{h_f,t} \sim \mathcal{N}(0,1),
\end{aligned} \tag{3}$$

where $k \in \{1, \ldots, N_j\}$ and $j \in \{1, \ldots, J\}$.

3.2 Priors

We pick loose priors for the model parameters to reduce the sensitivity of estimation results to the choice of prior distributions. More concretely, our priors exhibit symmetry across a range of empirical indicators related to geopolitical fragmentation $k \in \{1, ..., N_j\}$ and

$j \in \{1, \ldots, J\}$:

$$
\begin{aligned}
a_k^{(j)} = \begin{bmatrix} a_{k,0}^{(j)} \\ a_{k,1}^{(j)} \end{bmatrix} &\sim \mathcal{N}\left(\begin{bmatrix} 0 \\ 0 \end{bmatrix}, \begin{bmatrix} 1 & 0 \\ 0 & 1 \end{bmatrix} \right), \\
\rho_{u_k}^{(j)} &\sim \mathcal{N}\left(0, \frac{1}{100}\right), \\
(\sigma_{b_k}^{(j)})^2 &\sim \mathcal{IG}\left(100, 1\right), \\
(\sigma_g^{(j)})^2, \sigma_{h_f}^2 &\sim \mathcal{IG}\left(1, 1\right),
\end{aligned} \tag{4}
$$

where $g \in \{u_k, h_{u_k}, h_f\}$.

Our priors embody the belief that the degree of time variation in the factor loading $(\sigma_{b_k}^{(j)})^2$ is much smaller than the variations in the idiosyncratic error terms or the stochastic volatilities. However, for both cases, the weight of the prior relative to the sample for variances is not adjusted, leading to a substantial reduction in the impact of the prior as the sample length increases. We additionally explore a scenario wherein the factor loading $b_k^{(j)}$ remains constant over time, and we adopt a loose prior, which is centered around one with a substantial variance of $\mathcal{N}\left(1, \frac{1}{2}\right)$.

3.3 Estimation

The estimation of our dynamic hierarchical factor model employs a Gibbs sampler to draw samples from the exact finite-sample joint posterior distribution of both parameters and latent state variables, including the common factor. We extend the Gibbs sampler of Del Negro and Otrok (2008), addressing challenges related to missing data and discrepancies in data frequencies, particularly for stock variables rather than flow variables. Appendix B details our modifications.

We set the lag order for $u_{k,t}^{(j)}$ to one and define the time frame for our 16 indicators from 1975:Q1 to 2024:Q1. All indicators are standardized to zero mean and unit standard deviation to ensure comparability in measuring geopolitical fragmentation. The trade openness ratio, FDI ratio, financial flow ratio, migration flow ratio, and patent flows are multiplied by -1 to account for their inverse correlation with the underlying object of interest. This adjustment facilitates the imposition of symmetric priors for factor loadings across empirical indicators.

In instances where data are only accessible on an annual basis, the variables are characterized as stock rather than flow variables. Handling missing observations in this context is straightforward, as discussed in Aruoba et al. (2009). For the annual series, we assume that the individual error terms associated with them are not serially correlated.

In equation (3), there exist three sets of latent states: $\{f_t, f_t^{(j)}\}$, $\{b_{k,t}^{(j)}\}$, and $\{h_{f,t}, h_{f,t}^{(j)}, h_{u_k,t}^{(j)}\}$. All of these require initialization or normalization. To address the indeterminacy in the sign and magnitude of factor loadings $b_{k,t}^{(j)}$ and factor levels $f_t^{(j)}$, we initialize $b_{k,0}^{(j)}$ to a strictly

positive value, specifically 0.5. The initial values for f_t, $f_t^{(j)}$, $h_{f,t}$, $h_{f,t}^{(j)}$, and $h_{u_k,t}^{(j)}$ are set to zero, as their specific values are non-critical.

Additionally, we fix the variance of the innovation to the common factor to one ($\sigma_f^2 = 1$) and the variance of the innovation to the group-specific factor to one-tenth ($(\sigma_f^{(j)})^2 = 0.1$), reflecting our belief that group-specific variations are much smaller, as we aim to model significant comovement across groups. This belief is reinforced by fixing $\lambda^{(j)} = 1$, indicating that changes in the common factor translate into a one-to-one movement in the group-specific factors. While the specific values of $(\sigma_f^{(j)})^2$ are not critical for the median posterior estimates, they do influence the estimation uncertainty. Del Negro and Otrok (2008) provide a more detailed discussion on the identification of a DFM with time-varying loadings and stochastic volatilities, while Moench et al. (2013) address the identification of a DFM with a hierarchical structure.

3.4 Results

Figures 2 and 3 display the posterior median (smoothed) estimates of the common and group-specific geopolitical fragmentation factors, with 90% credible intervals. Major historical events affecting globalization are overlaid to aid interpretation.

Figure 2: Estimated common fragmentation factor

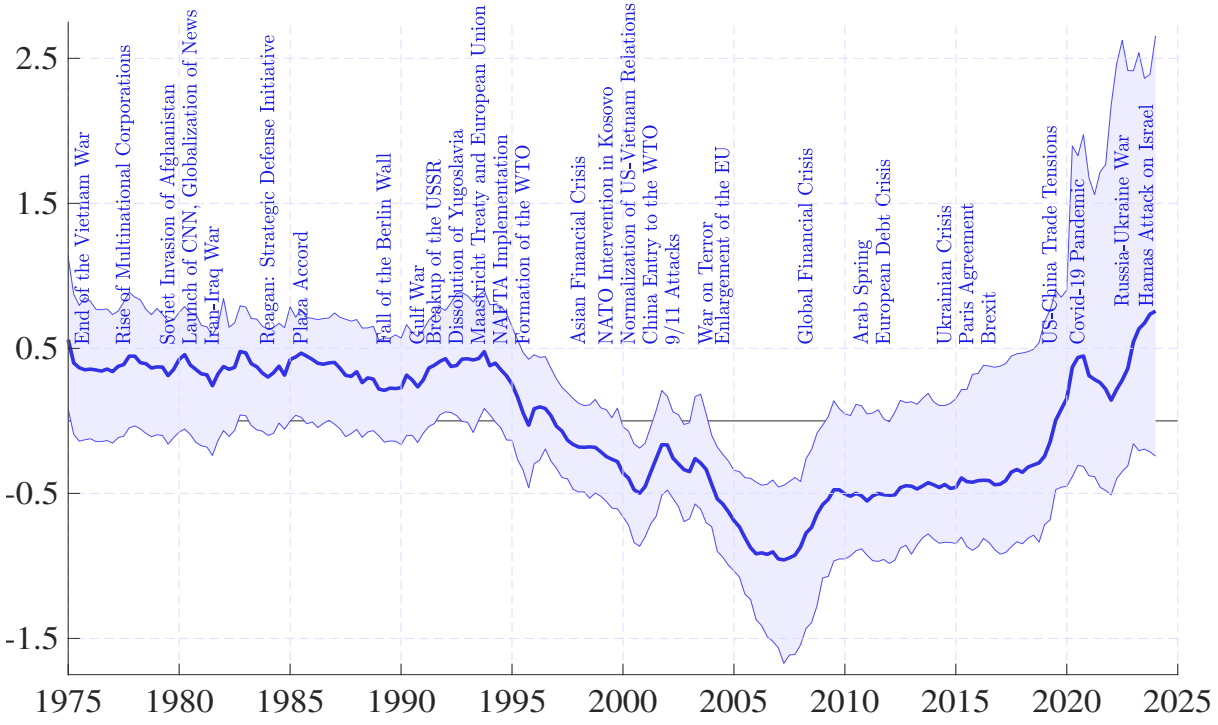

Notes: Posterior median-smoothed estimates of f_t accompanied by 90% credible intervals. Major historical events are overlaid.

Common geopolitical fragmentation factor

Our estimated common fragmentation factor, f_t, in Figure 2, aligns with the narrative understanding of geopolitical fragmentation outlined in Gopinath (2023). The median estimate remained stable from 1975 to the early 1990s. Although trade openness, FDI ratios, and financial flow rates increased during this period, they showed no strong upward trend, and the global economy remained divided between market and socialist blocs.

Our index shows globalization rising from the mid-1990s, driven by key events such as the Soviet Union's breakup, the Maastricht Treaty, the formation of the European Union, the establishment of the World Trade Organization (WTO), and China's WTO entry. Notably, this period also saw the term "globalization" gain popularity beyond economics.

This trend shifted post-2008, with a sharp rise during the 2007-2008 financial crisis. Between 2017 and 2020, geopolitical fragmentation accelerated due to mounting trade and capital flow challenges amid escalating geopolitical tensions and structural shifts. However, this upward momentum slowed between 2021 and 2022 as the worst effects of the COVID-19 pandemic subsided. From 2022 onward, fragmentation surged to unprecedented levels, driven by major geopolitical events, including Russia's invasion of Ukraine and the Hamas attack on Israel.

Group-specific geopolitical fragmentation factors

While the common geopolitical fragmentation index captures shared trends, group-specific factors highlight distinct dynamics within trade, financial, mobility, and political fragmentation. These factors help disentangle broader trends from the mechanisms driving each group's dynamics.

Figure 3 provides the posterior median (smoothed) estimates of $f_t^{(j)}$, our group-specific geopolitical fragmentation factors for $j \in \{\text{Trade, Financial, Mobility, Political}\}$, along with their 90% credible intervals. The blue line represents the common fragmentation factor, identical to Figure 2, while the orange lines (four in total) correspond to the hierarchical group-specific factors. These factors are jointly driven by the common fragmentation factor and subject to group-specific variations.

The key takeaway is that while substantial comovement exists across groups, group-specific fragmentation dynamics show notable heterogeneity. For instance, trade fragmentation declines more slowly than the common factor, falling below zero only around 2005, whereas the common factor began its decline around 1995. Moreover, trade fragmentation did not accelerate significantly post-2008 but has risen over the past eight years, coinciding with the Trump-era trade wars, increasing trade restrictions, new barriers, and heightened uncertainty. This period, described as "slowbalization" by Gopinath (2023) and Goldberg and Reed (2023), saw trade openness remain relatively flat since 2008 (until recent years)

Figure 3: Estimated group-specific fragmentation factors

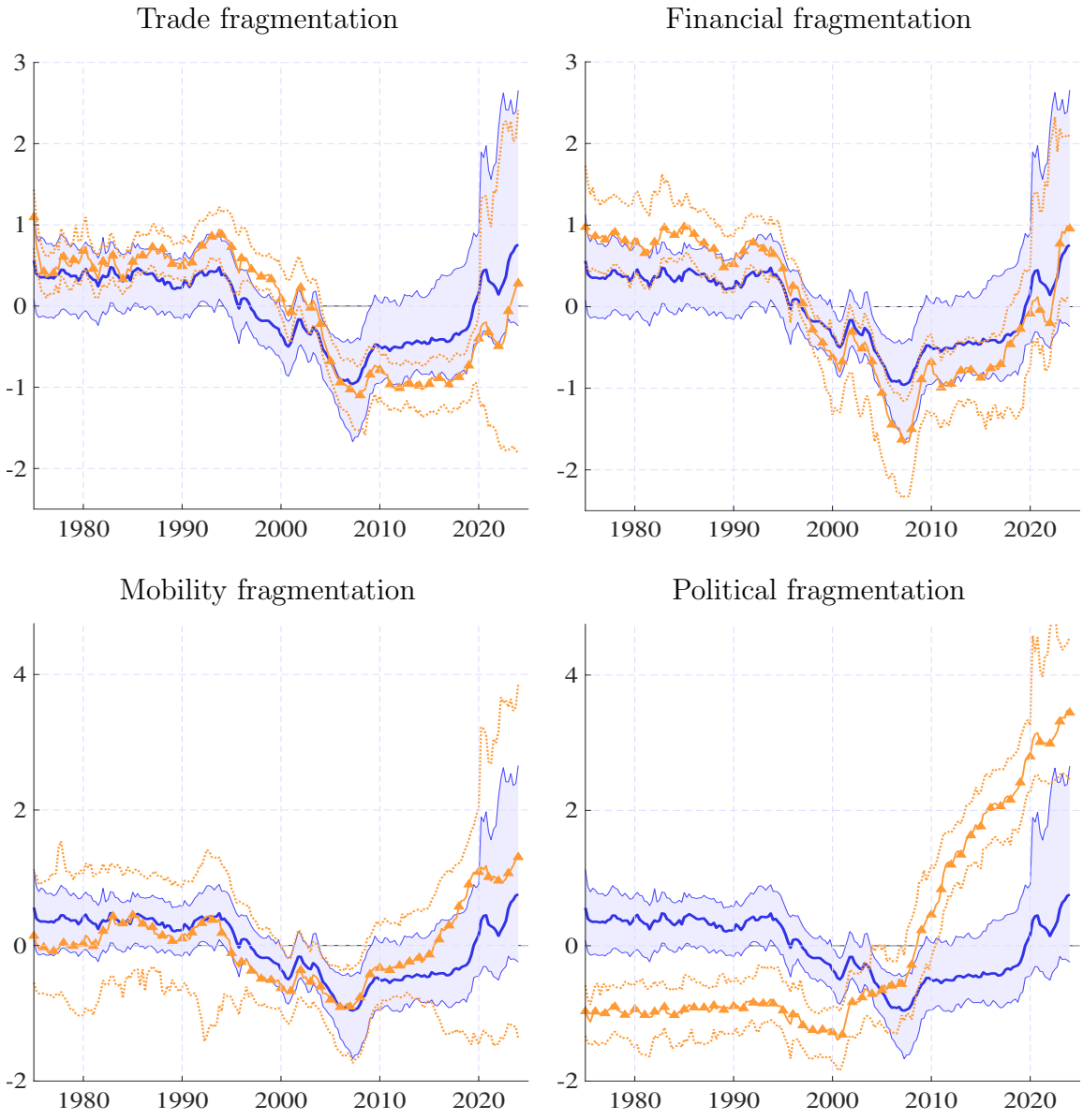

Notes: Posterior median-smoothed estimates of $f_t^{(j)}$ accompanied by 90% credible intervals, $j \in \{1, \ldots, J\}$. We overlay f_t with its 90% credible intervals, as shown in Figure 2.

rather than outright fragmentation. Our findings support this view and focusing solely on trade fragmentation leads to a similar conclusion.

In contrast, financial fragmentation, which reflects cross-border financial integration and restrictions, demonstrates very strong comovement with the common factor. The relationship is almost one-to-one, albeit with much higher volatility, yet still constrained by tight credible intervals. This suggests that financial fragmentation is a key driver of the common comovement.

Mobility fragmentation, which captures barriers to the physical and intellectual movement of people, shows no significant idiosyncratic movements. The 90% credible intervals are wide, and median values remain closely aligned with the common fragmentation index, indicating limited group-specific deviations.

The most striking result is in political fragmentation, which reflects global instability and institutional divergence. Unlike other groups, it sharply diverges from the common factor, surging post-2008. This rise coincides with sanctions, conflicts, and escalating geopolitical tensions, highlighting its accelerating role in recent years. Thus, political fragmentation emerges as a key driver of the sharp increase in the common geopolitical fragmentation factor over the past decade.

3.5 Robustness checks

In this section, we assess the robustness of our estimation by testing its consistency across different indicator classifications and evaluating the impact of specification choices. Specifically, we examine whether the results hold when using a simpler PCA-based approach instead of our more sophisticated factor model with time-varying parameters and stochastic volatility.

Robustness to group classification

In our baseline specification, we classify the empirical indicators into four groups: trade, financial, mobility, and political. While intuitive, we test whether our conclusions depend on this grouping by permuting indicator classifications into alternative groupings and re-estimating the model.

For ease of exposition, we re-categorize the empirical indicators into four areas:

(i) Metrics of economic integration: Trade Openness, FDI Ratio, Financial Flow Ratio, Migration Flow Ratio, Patent Flows.

(ii) Policy implementation gauges: Number of Trade Restrictions, Capital Control, Number of Sanctions, Temporary Trade Barriers, Tariff.

(iii) Text mining-derived indicators: Geopolitical Risk Index, Trade Policy Uncertainty, Energy Uncertainty, Migration Fear Index.

(iv) Political reflections: Number of Conflicts, UNGA Kappa Score.

This classification is plausible as it separates indicators of policy actions (e.g., trade restrictions) from those capturing policy outcomes (e.g., trade openness). Additionally, grouping fear or uncertainty indicators (e.g., geopolitical risk, and migration fear indices) into a separate category allows for an agnostic interpretation of whether they reflect outcomes or

policy influences. This approach clarifies distinctions between policy actions, outcomes, and perceptions (e.g., fear or uncertainty), providing an alternative perspective on how different indicators contribute to geopolitical fragmentation.

For this exercise, we propose a non-hierarchical DFM with two factors to test the robustness of the estimated common fragmentation dynamics to group classification. Introducing two factors is justified by our findings, which show strong comovement across group-specific factors while also revealing some heterogeneity. For $i \in 1, \ldots, N$ where $N = 16$,

$$
\begin{aligned}
y_{i,t} &= a_{i,t} + b_{i,t} f_{1,t} + c_{i,t} f_{2,t} + u_{i,t}, \\
a_{i,t} &= a_{i,0} + a_{i,1} t, \\
f_{1,t} &= \phi_{f_1} f_{1,t-1} + \sigma_{f_1,t} \epsilon_{f_1,t}, \quad \epsilon_{f_1,t} \sim \mathcal{N}(0,1), \\
f_{2,t} &= \phi_{f_2} f_{2,t-1} + \sigma_{f_2,t} \epsilon_{f_2,t}, \quad \epsilon_{f_2,t} \sim \mathcal{N}(0,1), \\
b_{i,t} &= b_{i,t-1} + \sigma_{b_i} \epsilon_{b_i,t}, \quad \epsilon_{b_i,t} \sim \mathcal{N}(0,1), \\
c_{i,t} &= c_{i,t-1} + \sigma_{c_i} \epsilon_{c_i,t}, \quad \epsilon_{c_i,t} \sim \mathcal{N}(0,1), \\
u_{i,t} &= \phi_{u_i} u_{i,t-1} + \sigma_{u_i,t} \epsilon_{u_i,t}, \quad \epsilon_{u_i,t} \sim \mathcal{N}(0,1), \\
h_{j,t} &= h_{j,t-1} + \sigma_{h_j} \epsilon_{h_j,t}, \quad \sigma_{j,t} = \sigma_j \exp(h_{j,t}), \quad \epsilon_{h_j,t} \sim \mathcal{N}(0,1).
\end{aligned} \tag{5}
$$

Although expanding the specification to three or more factors is possible, our results below show that it does not seem necessary. Appendix C describes the estimation process.

Estimating the DFM (5) requires identification assumptions on $b_{i,t}$ and $c_{i,t}$. These can be viewed as an exclusion restriction, where a subset of indicators loads exclusively on one factor. Without this, loadings could be arbitrarily reallocated between factors without affecting the overall likelihood. Additionally, a normalization is needed to distinguish both factors.

A simple and intuitive choice is to have all variables classified under "metrics of economic integration?" load on the first factor. We then explore all possible ways the remaining three categories ("policy implementation gauges," "text-mining-derived indicators," and "policy reflections") can load on both factors.[2] Ensuring each category loads on at least one factor and avoiding duplicates from label-switching yields 40 cases. One trivial case is when all four categories load only on the first factor, effectively reducing the model to a single-factor specification.[3]

Instead of reporting the results for each of the 40 cases, we select four representative cases described in Panel (B) of Figure 4 that are sufficient to make our point. Case ($I1$) implements the most extreme exclusion restrictions: the "metrics of economic integration" load exclusively on the first factor, while all other indicators load only on the second factor, ensuring

[2]The first category can also load on the second factor if another category is excluded from it.

[3]In principle, restricting individual components within each category would exponentially increase the number of cases. However, this approach seems more arbitrary than excluding entire categories and, given our findings, is unlikely to alter results.

Figure 4: Estimated factors under various identification assumptions on factor loadings

(A) Estimated factors

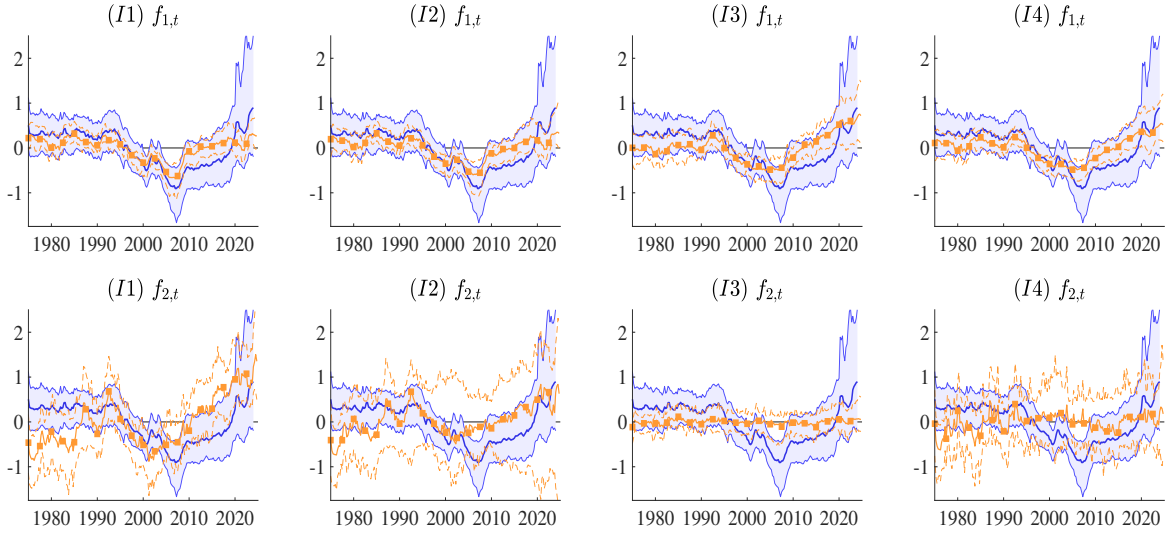

(B) Exclusion restrictions on factor loadings

Category	$(I1)$		$(I2)$		$(I3)$		$(I4)$	
	1^{st}	2^{nd}	1^{st}	2^{nd}	1^{st}	2^{nd}	1^{st}	2^{nd}
Metrics of economic integration	1	0	1	0	1	1	1	0
Policy implementation gauges	0	1	0	1	1	0	1	1
Text-mining-derived indicators	0	1	1	1	1	1	1	1
Political reflections	0	1	0	1	1	0	1	1

Notes: Panel (A) compares the estimates (indicated by red lines) with those from our baseline single-factor case, indicated by blue lines, as shown in Figure 2. For clarity, we label the two factors $f_{1,t}$ and $f_{2,t}$ as the 1^{st} and 2^{nd} factors, respectively. In panel (B), a value of 0 denotes an exclusion restriction applied during the estimation, indicating that the factor loading is set to zero for the corresponding entry.

no overlap between the two factors. Despite this separation, as shown in the first column of Panel (A) of Figure 4, each factor estimate still exhibits strong comovement with our baseline factor (depicted by the blue lines), albeit with varying levels of estimation uncertainty.

In contrast, cases $(I2)$, $(I3)$, and $(I4)$ are increasingly less restrictive, allowing some indicators to load on both factors. For instance, $(I2)$ also loads category "text-mining-derived indicators" on the first factor while $(I4)$ only excludes the first category "metrics of economic integration" from the second factor (the absolute minimal exclusion we can have to ensure identification). In these alternative cases, the second factor contributes minimally to the model, with the majority of the comovement captured by the first factor.

In summary, our findings confirm the robustness of estimating common fragmentation dynamics. The common geopolitical fragmentation factor remains consistent across different indicator classifications, reinforcing the validity of our results.

A PCA comparison

Our framework is a flexible framework that captures time variations, including changes in factor loadings and innovation variances. However, one might worry that its technical requirements, such as time-varying parameters and stochastic volatility, could obscure information that a simpler method like principal components analysis (PCA) might reveal more transparently. To ensure robustness, we compare our baseline results with those from PCA. While PCA effectively captures common fragmentation dynamics, it cannot account for the hierarchical structure central to our framework, underscoring the added value of our methodology.

Figure 5: Estimated common fragmentation factor derived from PCA

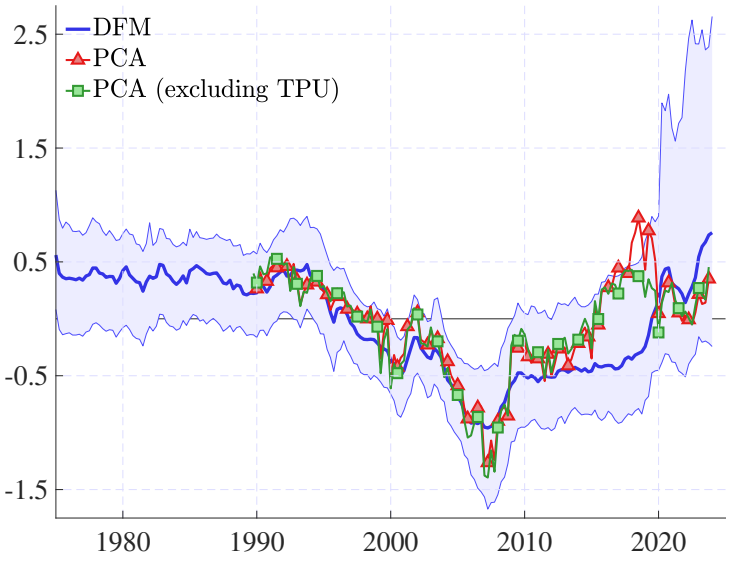

Notes: The exclusion of the initial seven years ($h = 10$ and $l = 5$) of data accounts for the missing data in the first PCA. We overlay f_t (blue line) with its 90% credible intervals, as shown in Figure 2.

To explore this idea, we follow Hamilton and Xi (2024), who propose a PCA procedure for extracting common cyclical factors from a mix of stationary and non-stationary variables. Using Hamilton (2018), we estimate an h-period-ahead forecast of each variable's level via OLS, regressing it on its own lags without requiring knowledge of its non-stationarity. We set h to 10 years and l to 5 years to estimate $y_{i,t+h} = \xi_0 + \sum_{j=1}^{l} \xi_j y_{i,t-j+1} + \nu_{i,t+h}$. We then compute the forecast errors as $\hat{\nu}_{i,t+h} = y_{i,t+h} - \hat{\xi}_0 - \sum_{j=1}^{l} \hat{\xi}_j y_{i,t-j+1}$ and apply PCA to these errors for the "Core 7" variables, following the method in Hamilton and Xi (2024). The Core 7—trade openness, the FDI ratio, the financial flow ratio, the number of sanctions, the geopolitical risk index, trade policy uncertainty, and the number of conflicts—are selected for their quarterly availability, unlike other indicators with only annual or inconsistent sample lengths. This constraint prevents us from applying PCA to the full indicator set used in our baseline framework.

Figure 5 presents the first principal component (red and green lines) alongside our baseline factor estimate (blue line). Both estimates exhibit similar patterns, including the decline in fragmentation starting in the mid-1990s and the subsequent increase following the 2007–2008 financial crisis. The overall correlation between the first principal component and the baseline estimate is approximately 0.73 when trade policy uncertainty (TPU) is included, increasing to 0.78 when TPU is excluded, likely due to the significant spike in TPU during 2018-2019. The primary difference lies in the sharper increase of the first principal component during 2015–2019, which we attribute to its heavy reliance on the Core 7 variables and the limited information available to the PCA procedure during this period.[4]

In sum, while the factor derived from PCA appears largely consistent, we retain the dynamic hierarchical factor model as our baseline specification because it seamlessly handles missing data and varying frequencies and provides the hierarchical structure needed to capture group-specific fragmentation dynamics.

3.6 Measuring geopolitical bloc fragmentation

Is global fragmentation evenly distributed across regions, or do certain areas experience it more acutely? An extreme case would be a world divided into distinct economic blocs, each operating under its own dynamics. While the global economy has not yet fully split into such blocs, measuring the extent of fragmentation between and within them is crucial.

Furthermore, to what extent does fragmentation within different geopolitical blocs shape their aggregate dynamics? How does regional fragmentation influence the global economy? To address these questions, we analyze fragmentation at the bloc level and assess its heterogeneous effects on global economic outcomes.

We analyze three geopolitical blocs: $j \in \{\text{U.S.-EU bloc}, \text{China-Russia bloc}, \text{Others bloc}\}$ using our baseline dynamic hierarchical factor model (3). Our bloc indicators capture fragmentation both within and across blocs.

The methodology follows the baseline approach, with adjustments for bloc-level data while ensuring consistency in other aspects. For each bloc, we compile eleven empirical indicators of geopolitical fragmentation, selected for relevance and data availability. These include trade openness, the FDI ratio, the financial flow ratio, the migration flow ratio, patent flow, temporary trade barriers, trade restrictions, capital control measures, sanctions, the geopolitical risk index, and the UNGA kappa score. Appendix A.5 provides further details.

[4]We also estimated the baseline model using the forecast errors, $\hat{\nu}_{i,t+h}$, by setting the deterministic time trend in (3) to zero. The correlation between these estimates and the baseline estimates is approximately 0.6. A notable issue with the approach à la Hamilton (2018) is the exclusion of the initial fifteen years of data, which leads to large and persistent credible intervals. These intervals expand further toward the end of the sample, particularly during the pandemic period. For brevity, these results are not reported here.

Figure 6: Estimated geopolitical bloc fragmentation indices

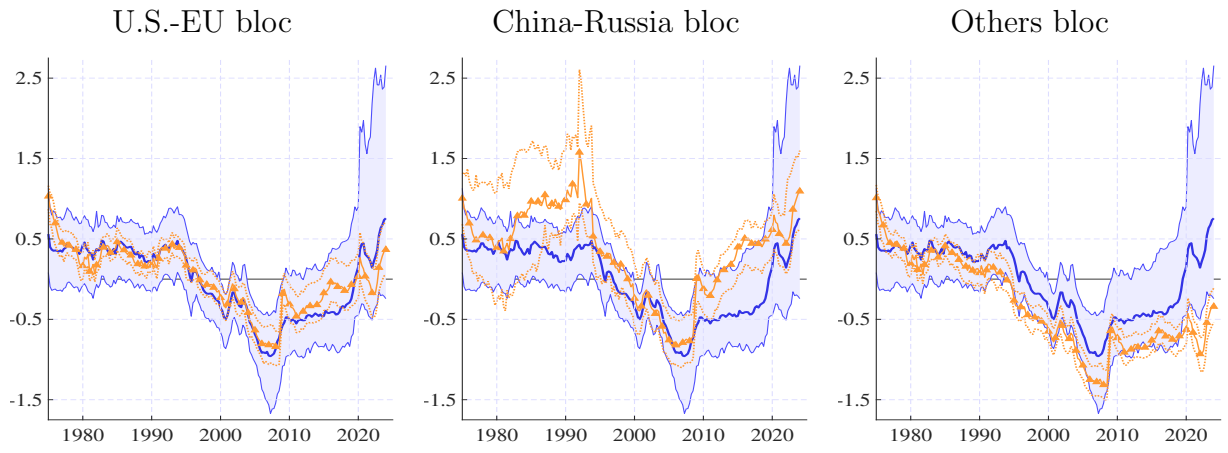

Notes: Posterior median-smoothed estimates of $f_t^{(j)}$ accompanied by 90% credible intervals where $j \in \{\text{U.S.-EU bloc}, \text{China-Russia bloc}, \text{Others bloc}\}$. We overlay f_t with its 90% credible intervals, as shown in Figure 2.

Figure 6 presents the estimated bloc fragmentation indices and their credible intervals, which broadly follow the global common fragmentation factor in Figure 2.[5] These indices reflect the globalization trend before the 2007-2008 financial crisis and the subsequent shift toward fragmentation. Here, "global" refers to indices constructed from data spanning all blocs rather than bloc-specific data. While these trends are shared, notable differences exist across geopolitical blocs.

Fragmentation patterns in the U.S.-EU bloc largely mirror the global common fragmentation factor, except in the past decade. Between 2016 and 2019, fragmentation rose more rapidly in this bloc but was less pronounced than the global trend from 2020 to 2024. These differences reflect bloc-specific dynamics despite broader similarities.

The globalization of the China-Russia and Others blocs also began in the mid-1990s, similar to the U.S.-EU bloc, driven by trade liberalization in large emerging economies. This trend was reinforced by regional trade agreements like NAFTA and Mercosur, alongside global institutions such as the WTO. Expanding trade and financial flows into emerging markets further supported globalization, but this trend reversed after the 2007-2008 financial crisis.

The China-Russia bloc shows a wider credible interval before the mid-1990s, reflecting limited data availability. More importantly, its fragmentation dynamics are shaped by the USSR's dissolution in 1991, China's transition toward a market economy, its WTO entry in 2001, and the gradual deregulation of capital flows. The fragmentation index for this bloc declines sharply from the early 1990s to 2007, signaling rapid integration.

[5]To ease interpretation, we compare them to the common fragmentation factor in Figure 2, despite having an alternative version based on eleven indicators for this exercise. In any case, both common factors exhibit a correlation above 0.9 and appear highly similar.

However, since the financial crisis, fragmentation has risen significantly faster in this bloc than in the U.S.-EU and Others blocs. This increase aligns with slowing trade and financial flows linked to China, including the 2018-2019 U.S.-China trade war, pushing fragmentation levels back to those of the early 1990s. The sharp rise in recent years is largely driven by Russia's 2022 invasion of Ukraine, which triggered widespread geopolitical and economic repercussions, including severe sanctions, economic decoupling from the West, and growing dependence on China for trade and financial partnerships.

The dynamics of the Others bloc differ in key ways. While fragmentation increased during the 2007-2008 financial crisis, it has remained relatively stable since, without substantial rises. This pattern reflects the bloc's reliance on commodity exports, which were heavily impacted by collapsing global demand during the crisis. Post-crisis, regional cooperation efforts, such as those led by ASEAN and the African Union, helped stabilize fragmentation levels. Trade substitution from China to other emerging economies, such as Mexico and Vietnam, following the U.S.-China trade war may have also contributed. Additionally, shifting trade patterns, including China's Belt and Road Initiative, fostered regional integration while bypassing global mechanisms.

The close alignment of the Others bloc's fragmentation dynamics with the global index suggests that, unlike the U.S.-EU or China-Russia blocs, these countries generally lack the geopolitical influence to shape global fragmentation actively. Instead, their dynamics primarily reflect responses to external shocks rather than deliberate policy actions.

4 The Causal Effects of Geopolitical Fragmentation

We now explore the causal link between geopolitical fragmentation and global economic activity. To assess causality in time series, we use structural vector autoregressions (SVARs) and local projections (LPs). Both estimate dynamic relationships among observed variables within a linear projection framework; see Plagborg-Møller and Wolf (2021). In finite samples and under model specification uncertainty, SVARs efficiently structure variable relationships, while LPs provide a more flexible framework, mitigating the curse of dimensionality. Their complementarities justify employing both approaches for a comprehensive assessment of geopolitical fragmentation's causal effects.

We apply SVARs and LPs to quarterly panel data covering 89 economies: 36 advanced economies (AEs) and 53 emerging markets (EMs) with available data. Appendix A.3 provides descriptive statistics for these variables.

We start with a panel SVAR to assess the impact of fragmentation on macroeconomic and financial variables. While our baseline analysis relies on the panel SVAR, we then transition to a panel LP framework to explore heterogeneity across country groups, shock types, and sectors.

4.1 The panel SVAR and LPs

The panel SVAR comprises 11 variables categorized into global and country components. The global bloc includes (i) our geopolitical fragmentation index, (ii) the VIX, (iii) the log of the S&P 500 index, (iv) the log of the WTI price of oil, (v) the yield on two-year U.S. Treasuries, (vi) the Chicago Federal Reserve National Financial Conditions Index (NFCI), and (vii) the log of world real GDP, aligning with the variable selection methodology of Caldara and Iacoviello (2022). The global variables control for the interactions between the fragmentation index and the aggregate variables of a country, aiding in the identification of the causal effects of shocks to the fragmentation index. Notably, U.S. financial market indicators are treated as "global" variables due to their influential role in the global market. The country bloc consists of (viii) the log of a country's stock price index (SP_{it}), (ix) the log of industrial production index (IP_{it}), (x) the log of fixed investment (I_{it}), and (xi) the log of per capita GDP (GDP_{it}).[6]

The SVAR includes two lags and uses quarterly data from 1986:Q1 to 2024:Q1, with the sample start determined by VIX availability. To account for country-specific factors, the panel SVAR is estimated with country fixed effects (FEs). Data come from the IMF International Financial Statistics (IFS), with observations in the top or bottom 0.5th percentile of period-over-period changes excluded as outliers. The unbalanced panel consists of 2,359 observations from 26 countries (17 AEs and 9 EMs). The sample size is smaller than in the LP analysis, as VARs require all variables to be available simultaneously.

In comparison, LPs can be executed for each variable independently, resulting in more observations for regressions. We implement a panel LP by estimating the following:

$$y_{i,t+h} - y_{i,t-1} = \beta^h s_t + \sum_{l=1}^{L} \alpha_l^h \Delta y_{i,t-l} + \sum_{l=1}^{L} \gamma_l^h s_{t-l} + \delta^h X_{i,t} + \mu_i^h + \epsilon_{i,t}^h, \tag{6}$$

for $h = 0, 1, 2, ...$ where $y_{i,t+h}$ represents the outcome variable in country i at time $t+h$, i.e., $y_{i,t+h} = \{\ln(\text{GDP}_{it+h}), \text{IP}_{it+h}, \ln(\text{I}_{it+h}), \ln(\text{SP}_{it+h})\}$, and s_t is the fragmentation shock obtained in the SVAR. Following Montiel Olea and Plagborg-Møller (2021), we include lagged outcome and explanatory variables, $\Delta y_{i,t-l}$ and s_{t-l}, to address serial correlation, choosing a lag length of two.

The regressor vector $X_{i,t}$ includes global and country-specific controls: the first and second lags of a country's per capita GDP growth rate and the global variables used in the VAR analysis –the VIX, the S&P 500 index, the WTI oil price, the yield on two-year U.S. Trea-

[6]For the panel VAR estimation, we construct for each country:

$$Y_{it}' = \begin{bmatrix} \text{Fragmentation Index}_t, & \text{VIX}_t, & \ln(\text{S\&P}_t), & \ln(\text{WTI}_t), & \text{U.S. Treasury}_t, & \text{NFCI}_t, \\ \ln(\text{World GDP}_t), & \ln(\text{SP}_{it}), & \text{IP}_{it}, & \ln(\text{I}_{it}), & \ln(\text{GDP}_{it}) & \end{bmatrix}.$$

suries, the NFCI, and world GDP. The WTI oil price and world GDP are in log-differences. We also include a dummy for 1996:Q1, as the SVAR leaves a fragmentation shock spike (3.3 standard deviations) that lacks a clear economic narrative. Finally, μ_i^h represents country FEs, and $\epsilon_{i,t}^h$ is the error term. Standard errors are clustered by time, as in the SVAR

The sequence of estimated coefficients, β^h for $h = 0, 1, 2,...$, represents the IRFs. The estimation period t extends until 2019:Q4 to ensure a consistent sample across h. We run the regression for each country variable separately. The number of observations differs across variables depending on data availability: 6,962 for GDP per capita (36 AEs and 53 EMs), 4,391 for industrial production, 6,189 for fixed investment, and 2,547 for stock prices in the longest horizon of the estimation ($h = 16$).

4.2 Establishing causality through various identification strategies

We consider three identification strategies for fragmentation shocks: Cholesky decomposition with varying variable orderings, a narrative approach, and a refinement using external controls.[7]

Our baseline case identifies fragmentation shocks using Cholesky decomposition, with the fragmentation index ordered first. This assumes geopolitical fragmentation is driven by low-frequency forces—such as demographic shifts, ideological changes, and political decisions—where legislative and engagement processes make it nearly infeasible to react to contemporaneous quarterly shocks in aggregate economic variables.

To test the robustness of this assumption, we reorder the Cholesky decomposition by placing the fragmentation index last. This alternative assumes fragmentation shocks have no contemporaneous effects on global or country-specific variables, representing a worst-case scenario for their significance.

Next, we apply narrative restrictions following Mertens and Ravn (2013). This approach identifies significant fragmentation and globalization episodes as external instruments for fragmentation shocks. To ensure orthogonality with other shocks, we select episodes that are unexpected or unrelated to the global economy's state. Thus, events directly tied to global economic conditions—such as the 2007-2008 financial crisis and the COVID-19 pandemic–are excluded.

Table 1 lists the selected narrative episodes, categorized into three sections, with comprehensive details provided in Appendix A.4. Episodes reflecting geopolitical fragmentation (globalization) are marked with an asterisk (dagger). We assign a value of 1 to fragmentation

[7]We avoid using a long-run identification strategy due to the lack of sharp theoretical predictions about the long-run effects of economic fragmentation. For instance, while economic theory often predicts that welfare (a non-observable) would decline with reduced international trade, observed output may rise or fall depending on factor endowments and relative prices. A similar argument precludes the use of heteroskedasticity-based identification strategies.

Table 1: Narrative episodes: Geopolitical fragmentation

(A) Surprise war outbreaks, international conflicts, terrorism
Iraqi invasion of Kuwait*(1990:Q3), Gulf War*(1991:Q1), NATO intervention in Serbia*(1994:Q2) and Kosovo*(1999:Q1), 9.11*(2001:Q3), Iraq War*(2003:Q1), U.S. strike on ISIL*(2014:Q3), Russia's invasion of Ukraine*(2022:Q1)
(B) Unforeseen geopolitical shifts
Geneva Accords between Afghanistan and Pakistan†(1988:Q2), Fall of the Berlin Wall†(1989:Q4), USSR dissolution events†(1988-1991), U.S.-Vietnam normalization†(1995:Q3), Arab Spring*(2010:Q4), Brexit vote*(2016:Q2)
(C) Enactment of trade deals, currency unions, or trade restrictions
NAFTA†(1994:Q1), WTO†(1995:Q1), Mercosur†(1995:Q1), Euro†(1999:Q1) and its expansion†(2004:Q2), U.S.-China trade war*(2018-2019)

Notes: See Table A-3 in Appendix A.4 for more details. We list 19 events, but we further break down historical occurrences, such as the dissolution of the USSR and the U.S.-China trade war, into multiple events. Hence, we present a total of 24 narrative episodes. Narrative episodes reflecting geopolitical fragmentation (globalization) are marked with an asterisk (dagger). For (C), while these events were typically agreed upon or announced beforehand, their implementation signifies material alterations in measures that impact economic activities. We verified that the exclusion of events under category (C) does not affect our result.

events and -1 to globalization events. Notably, the reduced-form residuals of the VAR model exhibit a correlation of approximately 0.15 with the narrative series.

Finally, the fragmentation shock identified through the baseline Cholesky decomposition is regressed on the military news shock from Ramey (2011) (updated in Ramey, 2016) and the monetary policy shock from Jarociński and Karadi (2020). This step addresses endogeneity concerns, as global variables in the panel SVAR may not fully control for it. We then use the resulting residuals as fragmentation shocks.[8]

4.3 Macroeconomic impact of common fragmentation shocks

We begin by examining impulse responses for all countries, focusing on shocks to the common fragmentation factor rather than group-specific factors.

[8]As discussed in Ramey (2016), shocks must meet three criteria to be exogenous: (1) they must be exogenous to current and lagged endogenous variables in the model, (2) they must be uncorrelated with other exogenous shocks to ensure identification of their unique causal effects, and (3) they must represent either unanticipated changes in exogenous variables or news about future movements in exogenous variables. We believe our residuals satisfy these conditions.

Aggregated impact across all countries

Panel (A) of Figure 7 presents impulse response functions (IRFs) of country-level variables to a one-standard-deviation fragmentation shock. Assuming identical coefficients across countries in the VAR system, these IRFs represent the average effects of a fragmentation shock within the sample. Following a positive innovation to the fragmentation index—interpreted as an adverse shock—all four country variables (GDP per capita, industrial production, fixed investment, and stock prices) decline. The negative effects peak one to two years after the initial shock and are both substantial and persistent. Notably, a one-standard-deviation fragmentation shock results in a peak GDP decline of about 0.4%.

As expected, the IRF magnitudes decrease compared to the baseline case, where the fragmentation index is ordered first in the Cholesky decomposition. Nonetheless, all variables except stock prices continue to show significant responses to fragmentation shocks, and the overall response patterns remain qualitatively unchanged. The lack of significance in stock prices likely reflects their forward-looking nature: they incorporate available information contemporaneously, reducing the effects of variables ordered later. Appendix D.2 confirms that results under alternative orderings fall between these two scenarios.

Panel (B) of Figure 7 depicts the IRFs when the fragmentation shock is instrumented using the narrative series. These impacts are substantially larger than those in the baseline case, with a one-standard-deviation shock leading to a 0.7% decline in GDP per capita. This result highlights potential measurement errors in the fragmentation index that are effectively mitigated by the narrative instruments.[9]

Panel (C) of Figure 7 presents the IRFs for a "cleaned" fragmentation shock, refined from the baseline Cholesky-identified shock using external control—the military news shock from Ramey (2011) (updated in Ramey, 2016) and the monetary policy shock from Jarociński and Karadi (2020). The adverse effects on country variables remain qualitatively similar to the baseline SVAR results. However, the estimated magnitudes align with the Cholesky case and are somewhat smaller than those from the narrative case. This difference is modest, given that LPs incorporate a broader EM sample and offer greater estimation flexibility.

Together, these three identification strategies—baseline Cholesky decomposition, narrative restrictions, and external control refinements—demonstrate the robustness of our results across a reasonable set of identification assumptions.

[9]The first-stage regression involves regressing the VAR reduced-form residuals on the narrative series: $u^f it = \underset{(0.012)}{-0.004} + \underset{(0.030)}{0.080}\ z_t + e_{it}$, where $u^f it$ represents the residuals of the fragmentation index from the panel VAR, and z_t is the narrative series. Standard errors, clustered by time, are reported in parentheses. The coefficient of the narrative series is significant at the 5% level. The second stage follows the steps outlined in Mertens and Ravn (2013).

Figure 7: Aggregate impact of fragmentation

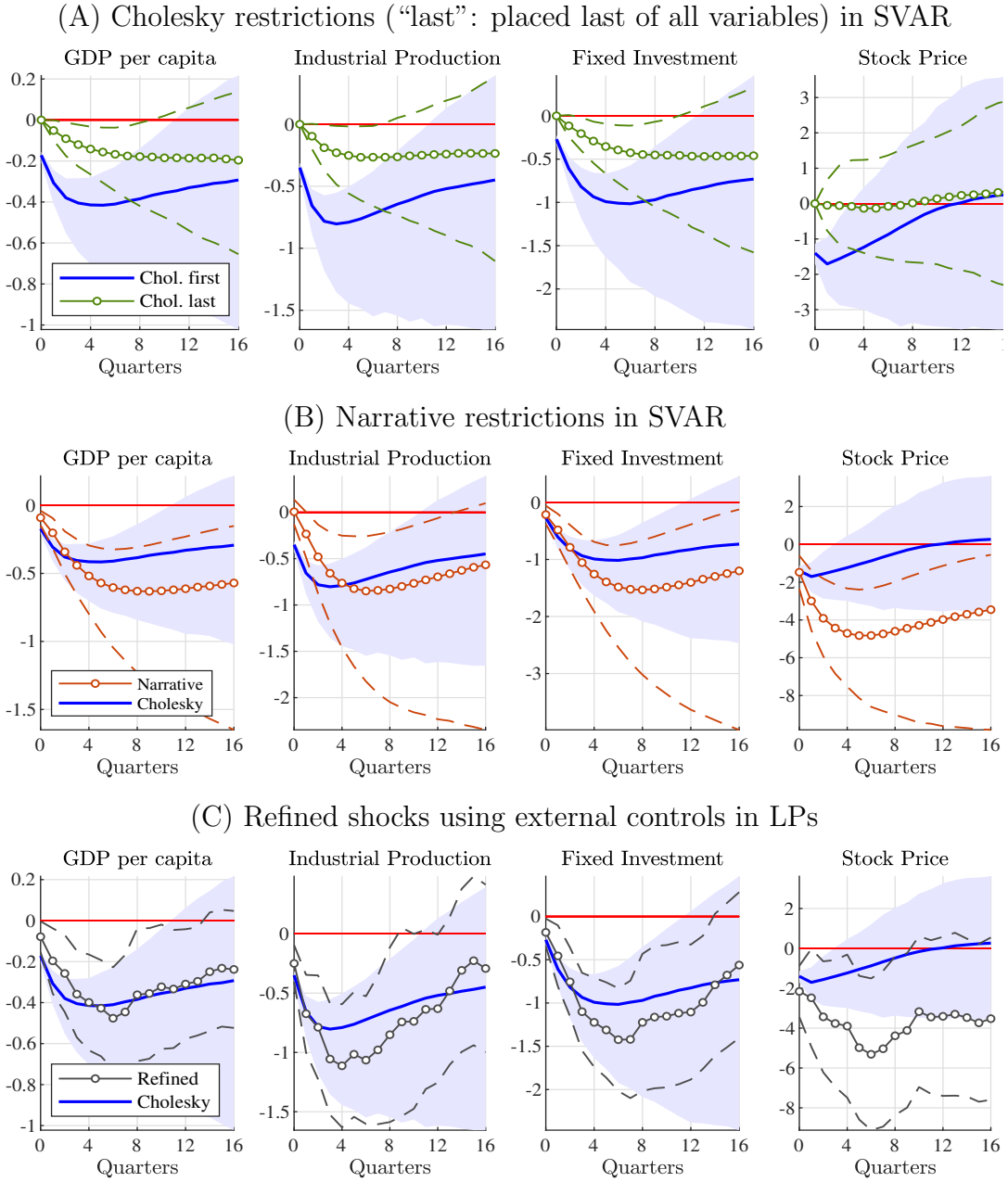

Notes: Sample of AEs and EMs. Percent responses to a one-standard-deviation fragmentation shock. Shaded (dashed) areas indicate the 90th percentiles, with standard errors clustered by time. Panel (A): Blue and green lines display the IRFs where the fragmentation index is ordered first and last in the Cholesky decomposition, respectively, while other variable orderings remain unchanged. Panel (B): The blue line shows the baseline case of the Cholesky decomposition with the fragmentation index ordered first. The red is obtained through the narrative restrictions described above. Panel (C): The fragmentation shock identified through the baseline Cholesky decomposition is regressed on the military news shock from Ramey (2011) (updated series from Ramey, 2016) and the monetary policy shock from Jarociński and Karadi (2020).

Figure 8: Disaggregated impact of fragmentation by country group, shock, and sector

(A) AEs (**red**) vs. EMs (**blue**)

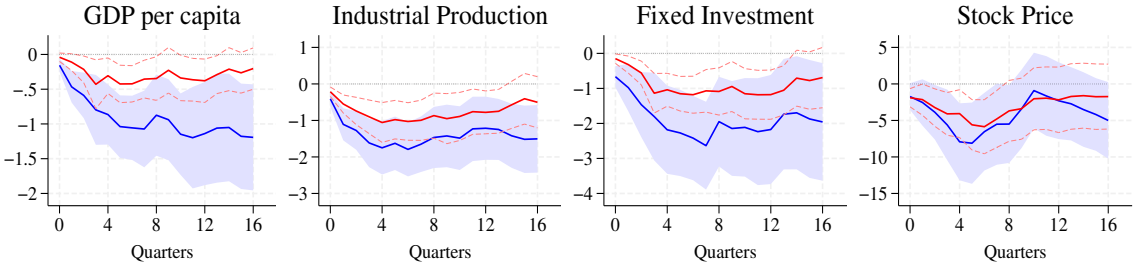

(B) Rising (**red**) vs. declining (**blue**) fragmentation shocks based on all countries

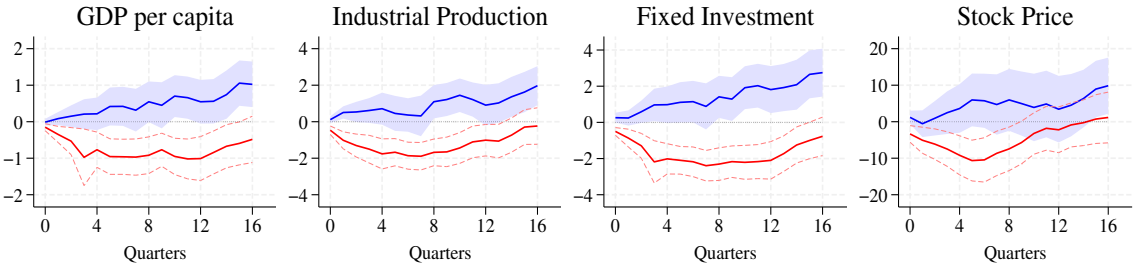

(C) Sectors in OECD countries

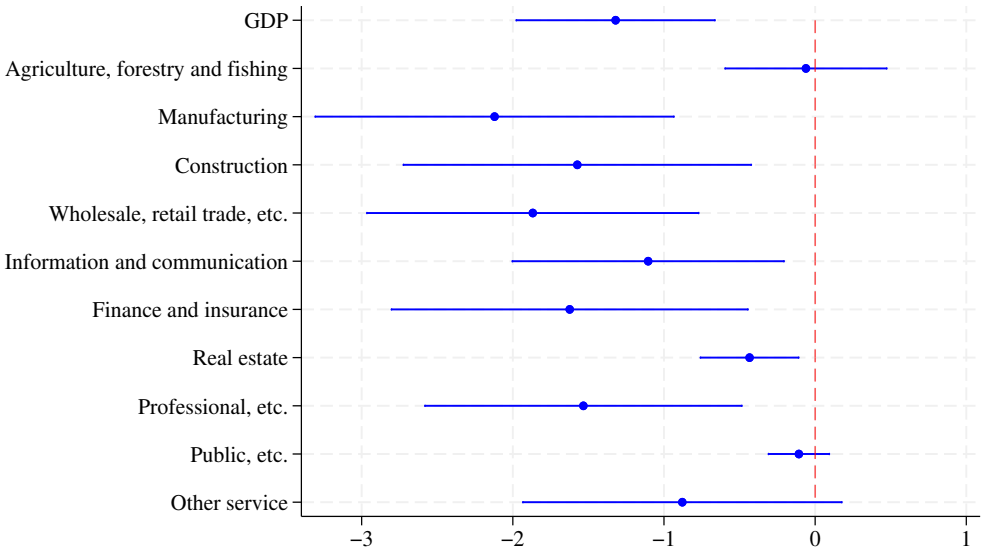

Notes: Percent responses to a one-standard-deviation fragmentation shock. Shaded areas and dashed lines indicate the 90th percentiles. In Panel (A), AEs and EMs follow the classification of the IMF World Economic Outlook. In Panel (B), a positive shock to the fragmentation index is denoted as a "rising" fragmentation shock, while a negative shock is referred to as a "declining" fragmentation shock. In Panel (C), we rely on 38 OECD countries. Percent responses of 1-year-ahead GDP to a one-standard-deviation shock to the factor. Bars indicate the 90th percentiles. "Wholesale, retail trade, etc." includes wholesale, retail trade, repairs, transport, accommodation, and food services. "Professional, etc." represents professional, scientific, and support services. "Public, etc." is the sum of public administration, defense, education, health, and social work.

Disaggregated impacts by country group, shock, and sector

We disaggregate results by country group, shock, and sector using LPs. Panel (A) of Figure 8 shows that fragmentation negatively affects both advanced economies (AEs) and emerging markets (EMs), with significantly stronger adverse effects on EMs. This suggests that lower-income countries are more vulnerable to fragmentation-induced disruptions, given their greater reliance on international economic linkages.

Panel (B) examines the differences between rising and declining fragmentation shocks by estimating their IRFs separately. The results show that rising fragmentation shocks have immediate adverse effects on the global economy, while declining fragmentation shocks unfold gradually over 2 to 3 years, exhibiting greater persistence.

Panel (C) of Figure 8 presents sectoral GDP responses to fragmentation shocks in OECD countries. Sectors more exposed to global economic and financial activities, such as manufacturing, finance and insurance, and construction (investment activities), exhibit stronger responses to fragmentation shocks. In contrast, domestically oriented sectors, including agriculture, forestry, fishing, real estate, and public services, show muted reactions.[10]

4.4 Macroeconomic impact of fragmentation shocks across groups and blocs

Across groups

Next, we analyze the implications of group-specific fragmentation dynamics for both common and group-specific factors. To identify group-specific fragmentation shocks, we use a combination of short-run zero restrictions and sign restrictions, following Binning (2013), consistent with the identification scheme in the dynamic hierarchical factor model.

We begin by estimating a VAR model, ordering the group-specific and common factors first, followed by the global control variables from Section 4.1. Group-specific fragmentation shocks are defined as those that increase (or decrease) the respective group-specific factor without affecting the common factor or other group-specific factors. The identification assumptions align with those for $\eta_t^{(j)}$ in our model.

In contrast, a common fragmentation shock increases both the common factor and all group-specific factors, corresponding to shocks to f_t in our model. These shocks are identified

[10]The OECD provides an annual GDP breakdown across ten major sectors for its 38 member countries. Using VAR-identified fragmentation shocks and the control variables outlined earlier, we conduct a panel LP analysis of (6). The dataset is an unbalanced panel spanning 1986 to 2023, with most countries' data available only from the late 1990s.

using the following zero and sign restrictions:

$$\begin{bmatrix} u_t^{\text{Trade}} \\ u_t^{\text{Financial}} \\ u_t^{\text{Mobility}} \\ u_t^{\text{Political}} \\ u_t^{\text{Common}} \\ \vdots \end{bmatrix} = \begin{bmatrix} \boldsymbol{+} & 0 & 0 & 0 & \boldsymbol{+} & \cdots \\ 0 & \boldsymbol{+} & 0 & 0 & \boldsymbol{+} & \cdots \\ 0 & 0 & \boldsymbol{+} & 0 & \boldsymbol{+} & \cdots \\ 0 & 0 & 0 & \boldsymbol{+} & \boldsymbol{+} & \cdots \\ 0 & 0 & 0 & 0 & \boldsymbol{+} & \cdots \\ \vdots & \vdots & \vdots & \vdots & \vdots & \ddots \end{bmatrix} \begin{bmatrix} \varepsilon_t^{\text{Trade}} \\ \varepsilon_t^{\text{Financial}} \\ \varepsilon_t^{\text{Mobility}} \\ \varepsilon_t^{\text{Political}} \\ \varepsilon_t^{\text{Common}} \\ \vdots \end{bmatrix}, \tag{7}$$

where $u_t^{(j)}$ represents the reduced-form residuals from the VAR, and $\varepsilon_t^{(j)}$ denotes bloc-driven fragmentation shocks. Sign restrictions are imposed for eight quarters after the shock, reflecting our assessment that low-frequency movements primarily drive fragmentation.

Then, the identified group-specific fragmentation shocks are added to the baseline panel VAR, replacing the global fragmentation index. Each group's shock is included in the VAR separately and is ordered first in the Cholesky decomposition for calculating the IRFs.[11]

Figure 9 presents the results. Due to our orthogonalization, where the primary effects operate through common fragmentation shocks, the macroeconomic impacts of group-specific fragmentation shocks are generally insignificant. For instance, trade-specific shocks initially lower GDP, industrial production (IP), fixed investment (FI), and stock prices (SP) but fade after a few quarters. Financial-specific fragmentation follows a similar pattern in the opposite direction, with positive immediate impacts that dissipate over time. Migration-specific shocks show little effect except for a notable impact on SP. The muted effects of group-specific shocks suggest that dynamics relevant to global economic activity are largely absorbed into the common fragmentation factor.

In contrast, political fragmentation shocks stand out, exhibiting persistent and additional negative effects on the global economy. This divergence likely reflects the nature of political fragmentation, which includes wars, military conflicts, and sanctions—events that severely disrupt global markets and depress SP, particularly stock prices. The results indicate that the rise in political fragmentation since the post-GFC period, as shown in Figure 3, has had distinct adverse effects on the global economy.

To test robustness, we explore alternative identification strategies. In this approach, group-specific fragmentation shocks are defined as those that increase (or decrease) both the respective group-specific factor and the common factor while leaving other group-specific factors unchanged. This strategy notably excludes a common shock. These refinements in

[11] The resulting VAR has 11 variables:

$$Y_{it}' = \begin{bmatrix} \varepsilon_t^{(j)}, & \text{VIX}_t, & \ln(\text{S\&P}_t), & \ln(\text{WTI}_t), & \text{U.S. Treasury}_t, & \text{NFCI}_t, \\ \ln(\text{World GDP}_t), & \ln(\text{SP}_{it}), & \ln(\text{IP}_{it}), & \ln(\text{I}_{it}), & \ln(\text{GDP}_{it}) & \end{bmatrix}$$

Figure 9: Economic impact of group-specific fragmentation: SVAR with zero/sign restrictions

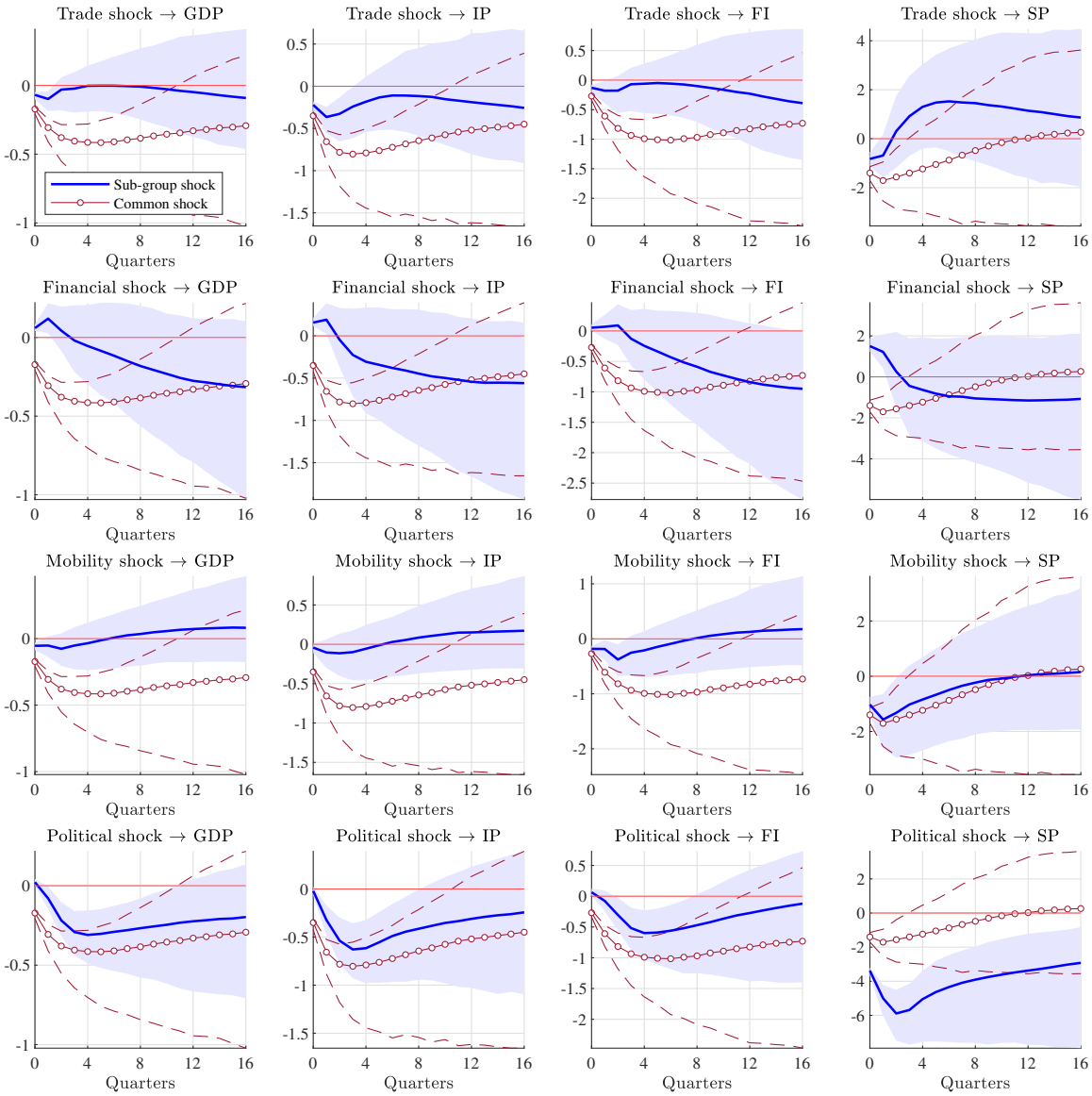

Notes: Sample of AEs and EMs. Percent responses to a one-standard-deviation shock. Shaded areas indicate the 90th percentiles where standard errors are clustered by time. Sub-group shocks are identified as those that have zero impacts on the common or other sub-group indices while increasing their own sub-group index in the 8-quarter horizon. The IRFs to the baseline global fragmentation shock (Cholesky decomposition) are shown in lines with circles as a reference.

restrictions ensure our findings remain robust under different identification assumptions.

The results for trade-, mobility-, and political-fragmentation shocks, shown in Appendix Figure A-6, remain consistent under this alternative identification strategy. However, for financial fragmentation shocks, the IRFs closely resemble those of common fragmentation shocks, reflecting the similarity between the estimated financial fragmentation factor and the common factor. Nonetheless, we retain our primary identification approach, as it aligns more

closely with our framework.

Across blocs

We use specification (7) to assess the macroeconomic impact of bloc-specific fragmentation shocks across countries. As shown in Figure 10, U.S.-EU and Others fragmentation shocks negatively affect the global economy. U.S.-EU shocks have immediate impacts, whereas Others shocks materialize in the medium run.

Figure 10: Economic impact of bloc-driven fragmentation: SVAR

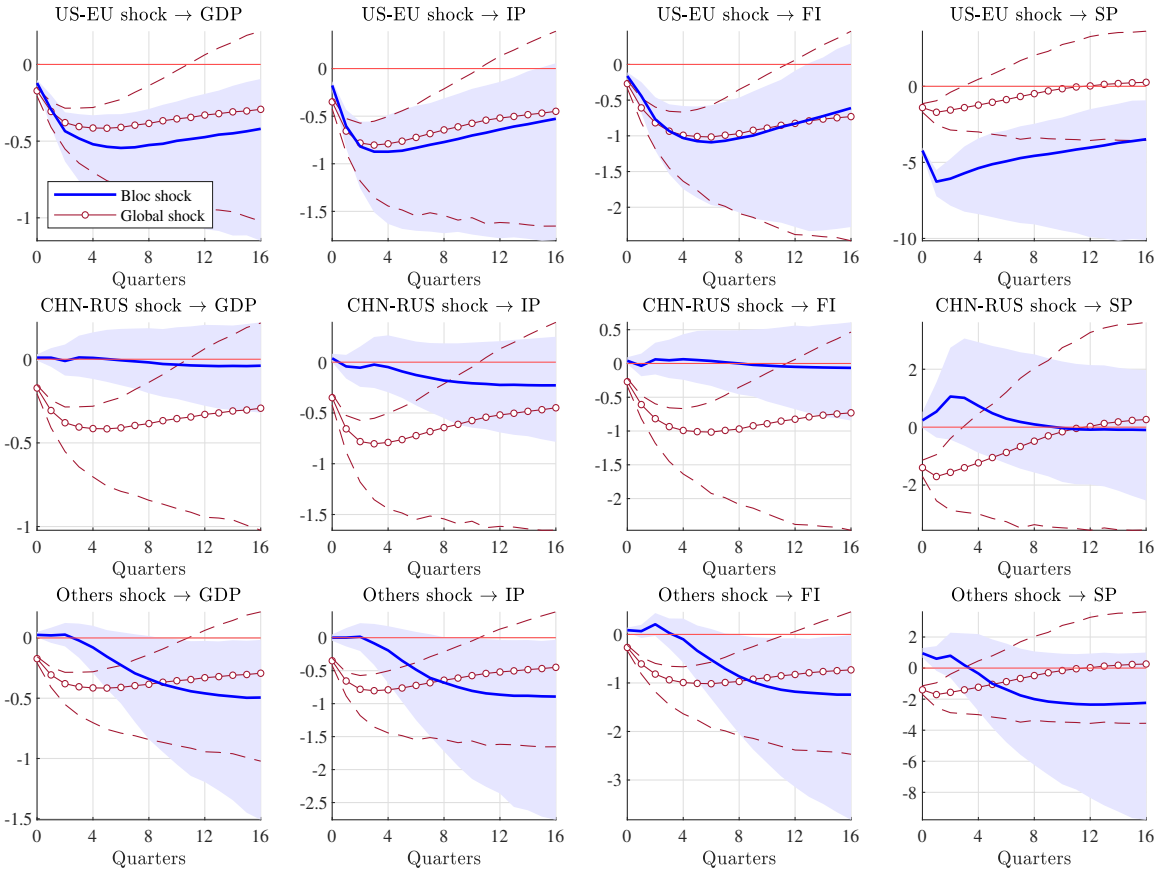

Notes: Sample of AEs and EMs. Percent responses to a one-standard-deviation shock. Shaded areas indicate the 90th percentiles where standard errors are clustered by time. The horizon of sign restrictions is set to 4 quarters. The IRFs to the baseline global fragmentation shock (Cholesky decomposition) are shown in gray as a reference.

In contrast, China-Russia fragmentation shocks show no significant effects over the analyzed horizons. This may suggest that China's global expansion has increased competition, partially substituting for other countries and offsetting effects. However, this finding should be interpreted cautiously, as our SVAR framework may not fully capture spillovers. For instance, the 2018-19 U.S.-China trade war likely led to trade relocation from China to other emerging economies, diluting the observable impact of China-Russia fragmentation shocks.

5 Conclusions

After decades of increasing global economic integration, recent trends indicate a shift toward fragmentation. However, measuring fragmentation presents a significant challenge. In this paper, we propose using a dynamic hierarchical factor model with time-varying parameters and stochastic volatility to integrate diverse empirical indicators and extract both a common fragmentation factor and four group-specific fragmentation factors.

We further demonstrate the usefulness of our estimation by applying it to causality assessments using SVARs and LPs. A one-standard-deviation shock to the fragmentation index negatively impacts the global economy, with emerging economies disproportionately affected. Notably, we identify an asymmetry: fragmentation exerts an immediate adverse effect on the global economy, whereas the benefits of reduced fragmentation, associated with globalization, materialize gradually. Additionally, our sectoral analysis shows that fragmentation disproportionately disrupts industries that are highly integrated into global markets, particularly manufacturing, construction, and finance.

References

Acemoglu, D., Gancia, G., and Zilibotti, F. (2015). Offshoring and directed technical change. *American Economic Journal: Macroeconomics*, 7:84–122.

Ahir, H., Bloom, N., and Furceri, D. (2022). The world uncertainty index. Working Paper 29763, National Bureau of Economic Research.

Aiyar, S., Chen, J., Ebeke, C., Ebeke, C. H., Garcia-Saltos, R., Gudmundsson, T., Ilyina, A., Kangur, A., Kunaratskul, T., Rodriguez, M. S. L., et al. (2023a). *Geo-economic Fragmentation and the Future of Multilateralism*. International Monetary Fund.

Aiyar, S., Presbitero, A., and Ruta, M. (2023b). *Geoeconomic Fragmentation: The Economic Risks from a Fractured World Economy*. CEPR Press.

Alesina, A. F., Furceri, D., Ostry, J. D., Papageorgiou, C., and Quinn, D. P. (2020). Structural reforms and elections: Evidence from a world-wide new dataset. Working Paper 26720, National Bureau of Economic Research.

Antràs, P. (2020). De-globalisation? Global value chains in the post-COVID-19 age. Mimeo.

Arias, J. E., Fernández-Villaverde, J., Rubio-Ramírez, J. F., and Shin, M. (2023). The causal effects of lockdown policies on health and macroeconomic outcomes. *American Economic Journal: Macroeconomics*, 15(3):287–319.

Aruoba, S. B., Diebold, F. X., and Scotti, C. (2009). Real-time measurement of business conditions. *Journal of Business and Economic Statistics*, 27(4):417–427.

Attinasi, M. G., Boeckelmann, L., and Meunier, B. (2023). The economic costs of supply chain decoupling. ECB Working Paper No. 2023/2839.

Bai, X., Fernández-Villaverde, J., Li, Y., and Zanetti, F. (2024). The causal effects of global supply chain disruptions on macroeconomic outcomes: Evidence and theory. Working Paper 32098, National Bureau of Economic Research.

Baker, M. and Wurgler, J. (2007). Investor sentiment in the stock market. *Journal of Economic Perspectives*, 21(2):129–152.

Baker, S. R., Bloom, N., and Davis, S. J. (2016). Measuring economic policy uncertainty. *Quarterly Journal of Economics*, 131(4):1593–1636.

Bartelme, D. and Gorodnichenko, Y. (2015). Linkages and economic development. Working Paper 21251, National Bureau of Economic Research.

Binning, A. (2013). Underidentified SVAR models: A framework for combining short and long-run restrictions with sign-restrictions. Norges Bank Working Paper No.2013/14.

Blanga-Gubbay, M. and Rubinova, S. (2023). Is the global economy fragmenting? World Trade Organization Staff Working Paper 2023-10.

Bloom, N., Bunn, P., Chen, S., Mizen, P., Smietanka, P., and Thwaites, G. (2019). The impact of Brexit on UK firms. Working Paper 26218, National Bureau of Economic Research.

Bloom, N., Davis, S., and Baker, S. (2015). Immigration fears and policy uncertainty. VOXEU Column, 15 December, 2015.

Bolhuis, M. A., Chen, J., and Kett, B. (2023). Fragmentation in global trade: Accounting for commodities. IMF Working Paper WP/23/73, International Monetary Fund.

Bown, C., Cieszkowsky, M., Erbahar, A., and Signoret, J. (2020). Temporary Trade Barriers Database. Washington, DC: World Bank.

Bustos, P. (2011). Trade liberalization, exports, and technology upgrading: Evidence on the impact of MERCOSUR on Argentinian firms. *American Economic Review*, 101:304–340.

Caldara, D. and Iacoviello, M. (2022). Measuring geopolitical risk. *American Economic Review*, 112(4):1194–1225.

Caldara, D., Iacoviello, M., Molligo, P., Prestipino, A., and Raffo, A. (2020). The economic effects of trade policy uncertainty. *Journal of Monetary Economics*, 109:38–59.

Campos, R. G., Estefania-Flores, J., Furceri, D., and Timin, J. (2023). Geopolitical fragmentation and trade. *Journal of Comparative Economics*, 51(4):1289–1315.

Carter, C. K. and Kohn, R. (1994). On Gibbs sampling for state space models. *Biometrika*, 81(3):541–553.

Cerdeiro, D. A., Eugster, J., Mano, R. C., Muir, D., and Peiris, S. J. (2021). Sizing up the effects of technological decoupling. IMF Working Paper, WP/21/69.

Clayton, C., Maggiori, M., and Schreger, J. (2024). A theory of economic coercion and fragmentation. Manuscript.

Dang, T. H.-N., Nguyen, C. P., Lee, G. S., Nguyen, B. Q., and Le, T. T. (2023). Measuring the energy-related uncertainty index. *Energy Economics*, 124(106817).

Del Negro, M. and Otrok, C. (2008). Dynamic factor models with time-varying parameters: Measuring changes in international business cycles. *Federal Reserve Bank of New York Staff Reports no. 326*.

Del Negro, M. and Schorfheide, F. (2011). Bayesian macroeconometrics. In Geweke, J., Koop, G., and van Dijk, H., editors, *The Oxford Handbook of Bayesian Econometrics*, pages 293–389. Oxford University Press.

Durbin, J. and Koopman, S. J. (2001). *Time Series Analysis by State Space Methods*. Oxford University Press.

Erten, B., Korinek, A., and Ocampo, J. A. (2021). Capital controls: Theory and evidence. *Journal of Economic Literature*, 59(1):45–89.

Fajgelbaum, P. D., Goldberg, P. K., Kennedy, P. J., and Khandelwal, A. K. (2019). Return to protectionism. *Quarterly Journal of Economics*, 135:1–55.

Fajgelbaum, P. D. and Khandelwal, A. K. (2022). The economic impacts of the US–China trade war. *Annual Review of Economics*, 14:205–228.

Feenstra, R. C. (2006). New evidence on the gains from trade. *Review of World Economics / Weltwirtschaftliches Archiv*, 142(4):617–641.

Felbermayr, G., Kirilakha, A., Syropoulos, C., Yalcin, E., and Yotov, Y. V. (2020). The global sanctions data base. *European Economic Review*, 129:103561.

Fernández, A., Klein, M. W., Rebucci, A., Schindler, M., and Uribe, M. (2016). Capital control measures: A new dataset. *IMF Economic Review*, 64:548–574.

Flaaen, A. and Pierce, J. (2019). Disentangling the effects of the 2018-2019 tariffs on a globally connected U.S. manufacturing sector. Finance and Economics Discussion Series 2019-086, Federal Reserve Board.

Frankel, J. A. and Romer, D. H. (1999). Does trade cause growth? *American Economic Review*, 89(3):379–399.

Geweke, J. (1977). The dynamic factor analysis of economic time series. In Aigner, D. J. and Goldberger, A. S., editors, *Latent Variables in Socio-Economic Models*, chapter 19. North Holland, Amsterdam.

Geweke, J. and Zhou, G. (1996). Measuring the pricing error of the arbitrage pricing theory. *Review of Financial Studies*, 9(2):557–587.

Gilchrist, S. and Zakrajšek, E. (2012). Credit spreads and business cycle fluctuations. *American Economic Review*, 102(4):1692–1720.

Glennon, B. (2024). How do restrictions on high-skilled immigration affect offshoring? Evidence from the H-1B program. *Management Science*, 70:907–930.

Góes, C. and Bekkers, E. (2022). The impact of geopolitical conflicts on trade, growth, and innovation. World Trade Organization, Staff Working Paper ERSD-2022-09.

Goldberg, P. and Reed, T. (2023). Is the global economy deglobalizing? *Brookings Papers on Economic Activity Spring*, 2023(2).

Gopinath, G. (2023). Cold War II? Preserving economic cooperation amid geoeconomic fragmentation. Plenary Speech at the 20th World Congress of the International Economic Association, Colombia, December 11, 2023.

Gopinath, G., Gourinchas, P.-O., Presbitero, A. F., and Topalova, P. (2025). Changing global linkages: A new Cold War? *Journal of International Economics*, 153:104042.

Häge, F. M. (2017). Chance-corrected measures of foreign policy similarity (FPSIM Version 2). Harvard Dataverse, V2.

Hakobyan, S., Meleshchuk, S., and Zymek, R. (2023). Divided we fall: Differential exposure to geopolitical fragmentation in trade. IMF Working Paper No. 2023/270.

Hamilton, J. D. (2018). Why you should never use the Hodrick-Prescott filter. *Review of Economics and Statistics*, 100(5):831–843.

Hamilton, J. D. and Xi, J. (2024). Principal component analysis for nonstationary series. Manuscript.

Jarociński, M. and Karadi, P. (2020). Deconstructing monetary policy surprises—the role of information shocks. *American Economic Journal: Macroeconomics*, 12:1–43.

Javorcik, B. S., Kitzmueller, L., Schweiger, H., and Yıldırım, M. A. (2024). Economic costs of friendshoring. *The World Economy*, 00:1–38.

Jurado, K., Ludvigson, S. C., and Ng, S. (2015). Measuring uncertainty. *American Economic Review*, 105(3):1177–1216.

Kim, S., Shephard, N., and Chib, S. (1998). Stochastic volatility: Likelihood inference and comparison with ARCH models. *Review of Economic Studies*, 65(3):361–393.

LaBelle, J., Martinez-Zarzoso, I., Santacreu, A. M., and Yotov, Y. (2023). Cross-border patenting, globalization, and development. Federal Reserve Bank of St. Louis Working Paper 2023-031.

Melitz, M. J. and Trefler, D. (2012). Gains from trade when firms matter. *Journal of Economic Perspectives*, 26(2):91–118.

Mertens, K. and Ravn, M. O. (2013). The dynamic effects of personal and corporate income tax changes in the United States. *American Economic Review*, 103(4):1212–1247.

Moench, E., Ng, S., and Potter, S. (2013). Dynamic hierarchical factor models. *Review of Economics and Statistics*, 95(5):1811–1817.

Montiel Olea, J. L. and Plagborg-Møller, M. (2021). Local projection inference is simpler and more robust than you think. *Econometrica*, 89(4):1789–1823.

Obstfeld, M. (1994). Risk-taking, global diversification, and growth. *American Economic Review*, 84:1310–1329.

Otrok, C. and Whiteman, C. H. (1998). Bayesian leading indicators: Measuring and predicting economic conditions in Iowa. *International Economic Review*, 39(4):997–1014.

Plagborg-Møller, M. and Wolf, C. K. (2021). Local projection and VARs estimate the same impulse. *Econometrica*, 89(2):955–980.

Ramey, V. A. (2011). Identifying government spending shocks: It's all in the timing. *Quarterly Journal of Economics*, 126:1–50.

Ramey, V. A. (2016). Macroeconomic shocks and their propagation. In Taylor, J. B. and Uhlig, H., editors, *Handbook of Macroeconomics*, volume 2, page 71–162. Elsevier B.V.

Sampson, T. (2017). Brexit: The economics of international disintegration. *Journal of Economic Perspectives*, 31:163–184.

Sargent, T. J. and Sims, C. A. (1977). Business cycle modeling without pretending to have too much a priori economic theory. In *New Methods in Business Cycle Research*. FRB Minneapolis, Minneapolis.

Shapiro, A. H., Sudhof, M., and Wilson, D. J. (2022). Measuring news sentiment. *Journal of Econometrics*, 228(2):221–243.

Stock, J. H. and Watson, M. W. (1989). New indices of coincident and leading economic indicators. In Blanchard, O. J. and Fischer, S., editors, *NBER Macroeconomics Annual 1989*, volume 4, pages 351–394. MIT Press, Cambridge.

Utar, H., Ruiz, L. B. T., and Zurita, A. C. (2023). The US-China trade war and the relocation of global value chains to Mexico. CESifo Working Paper No. 10638.

Wu, J. C. and Xia, F. D. (2016). Measuring the macroeconomic impact of monetary policy at the zero lower bound. *Journal of Money, Credit and Banking*, 48(2-3):253–291.

Online Appendix

A Data

A.1 Geopolitical fragmentation indicators

Descriptions and data sources are found below.

1. **The trade openness ratio**
   Description. The trade openness ratio is defined as the sum of exports and imports of goods and services divided by nominal GDP. The global indicator is constructed as the sum of all countries' exports and imports divided by world nominal GDP in current U.S.$. The definition is isomorphic to a country's trade openness weighted by the nominal GDP share. The bloc indicators are calculated accordingly for a group of countries in each bloc.
   Frequency. Quarterly.
   Sources. Exports and imports are obtained from the balance of payment (BoP) statistics in the International Financial Statistics (IFS). GDP is also taken from the IFS, and missing values are imputed by the linear interpolation of the annual GDP series in the World Economic Outlook (WEO) Database. Since Chinese trade data have a limited period (since 2005:Q1) in the IFS, they are imputed by trade partners' exports and imports available in the IMF Direction of Trade Statistics.

2. **The number of trade restrictions**
   Description. The Global Trade Alert (GTA) compiles a government statement that includes a credible announcement of a meaningful and unilateral change in the relative treatment of foreign vs. domestic commercial interests. The foreign commercial interests considered by the GTA are trade in goods and services, investment, and labor force migration. All documented changes reflect unilateral government action and exclude changes coordinated within bilateral trade agreements or the multilateral trading system. We count the number of announcements made (with equal weights), since the information regarding the magnitude of their economic impacts is not available. Bloc indicators are the sum of the announcements made by countries in each bloc.
   Frequency. Monthly data are converted to quarterly series.
   Source. Data are obtained from the Global Trade Alert.

3. **The temporary trade barriers**
   Description. The Temporary Trade Barriers (TTB) database, compiled by Bown et al. (2020), collects antidumping, countervailing, and safeguard measures across over 30

countries from the 1980s through 2019. These policy measures, often referred to as trade remedy actions, are implemented by government authorities against imports likely to have an adverse effect on national production, either by dumping, subsidies, or import surges by foreign sellers. These actions are collected at a detailed level, drawing on notifications, as wells as on national investigation case documents, in the interest of increasing transparency as to these trade policy actions. We count the implementation of temporary trade barriers. Bloc indicators are the number of those implemented in each bloc. While the country coverage is narrower than the GTA, the TTB spans a longer time series.

Frequency. Monthly data are converted to quarterly series.

Source. The data are downloaded from the database built by Bown et al. (2020).

4. **The trade policy uncertainty**

   Description. The trade policy uncertainty (TPU) index is based on the frequency of joint occurrences of trade policy and uncertainty terms across major newspapers.[1] It covers seven newspapers: Boston Globe, Chicago Tribune, Guardian, Los Angeles Times, New York Times, Wall Street Journal, and Washington Post. The index is calculated by counting the monthly frequency of articles discussing trade policy uncertainty (as a share of the total number of news articles) for each newspaper. The index is then normalized to 0 for a 1% article share. No country-specific or bloc indicators are available.

   Frequency. Monthly data are converted to quarterly series.

   Source. Caldara et al. (2020). The extended series is available on the website.

5. **Tariffs**

   Description. Alesina et al. (2020) created a comprehensive tariff measure, a weighted average of effective tariffs. The main data sources are the World Integrated Trade Solution (WITS) and World Development Indicators (WDI), covering data from 1988 to 2014. Other sources include the World Trade Organization (WTO) for the period 1993-2014; the General Agreement on Tariffs and Trade (GATT) for the period 1978-1987; and the Brussels Customs Union database (BTN) for the period 1966-1995. The global indicator is constructed as the PPP GDP weighted average of the whole sample, whereas bloc indicators are calculated accordingly in each bloc.

   Frequency. Annual.

   Source. The data are downloaded from the database built by Alesina et al. (2020).

6. **The FDI ratio**

   Description. The foreign direct investment (FDI) ratio is the sum of FDI inflows and

[1] Caldara et al. (2020) constructed indicators from newspaper coverage, firms' earnings calls, and tariff rates. We use the one based on newspaper coverage, which was updated in recent months.

outflows in the BoP statistics divided by nominal GDP. The global and bloc indicators are constructed in the same way as the trade openness ratio.

Frequency. Quarterly.

Sources. The IFS and WEO database. The same as the trade openness ratio.

7. **The financial flow ratio**

   Description. The financial flow ratio is calculated as the sum of inflows and outflows associated with portfolio investment and other investments in the BoP statistics as a share of nominal GDP. The global indicator and bloc indicators are constructed in the same way as the trade openness ratio.

   Frequency. Quarterly.

   Sources. The IFS and WEO database. The same as the trade openness ratio.

8. **The capital control measure**

   Description. We follow Fernández et al. (2016) for the definition of capital control measures. The IMF's Annual Report on Exchange Arrangements and Exchange Restrictions (AREAER) reports the presence of rules and regulations for international transactions by asset categories for each country. Fernández et al. (2016) use the narrative description in the AREAER to determine whether there are restrictions on international transactions, with 1 representing the presence of a restriction and 0 representing no restriction according to several rules. For instance, if the narrative of control involves "authorization," "approval," "permission," or "clearance," from a public institution, the control is deemed to be in place, while it is not if a requirement is "reporting," "registration," or "notification." A quantity restriction on investment (e.g., "ceiling") is regarded as a control. Also, suppose restrictions are imposed on sectors that are not deemed to have a macroeconomic effect or are associated with a particular country or small group of countries for non-macroeconomic reasons. In that case, they are not categorized as capital controls. They construct 1 or 0 indicators in each country for inflows and outflows of 10 asset categories (equity, bonds, money market instruments, collective investment, financial credits, foreign direct investment, derivatives, commercial credits, financial guarantees, and real estate). A country indicator is calculated as the average of the 20 sub-indicators. The global and bloc indicators are calculated as the weighted average of a respective group of countries using PPP GDP weights. The index does not take into consideration controls related to sanctions or national security reasons.

   Frequency. Annual.

   Sources. Fernández et al. (2016). The extended series, updated on August 12, 2021, is available on the website. PPP GDP is obtained from the WEO Database.

9. **The migration flow ratio**

   Description. Migration flows are defined as the absolute number of net migration flows in each country as a share of the population. The global and bloc indicators are calculated as the weighted average of a respective group of countries using population weights.

   Frequency. Annual.

   Sources. Data are obtained from the World Population Prospects 2022 by the United Nations.

10. **The patent flows**

    Description. Cross-border patents are those filed in one country by a resident of another. Patent data are from International Patent and Citations across Sectors (INPACT-S) compiled by LaBelle et al. (2023). The database is based on PATSTAT Global Autumn 2021 –a commonly used patent dataset– but LaBelle et al. (2023) impute missing data using available information and recover a large number of observations. The global and bloc indicators are calculated as the sum of a respective group of countries.

    Frequency. Annual.

    Sources. Data are obtained from INPACT-S compiled by LaBelle et al. (2023).

11. **The migration fear index**

    Description. The migration fear index is constructed by counting the number of newspaper articles with at least one term related to migration (e.g., "border control") and fear (e.g., "fear," "concern"), and then dividing by the total count of newspaper articles. The index is available for four countries: the UK, Germany, France, and the U.S. The global index is a simple average of these countries' standardized indices.

    Frequency. Monthly data are converted to quarterly series.

    Source. Bloom et al. (2015). The series is downloaded from the website.

12. **The geopolitical risk index**

    Description. The geopolitical risk (GPR) index provides a news-based measure of adverse geopolitical events and associated risks. It is constructed by counting the number of articles related to adverse geopolitical events in each newspaper each month as a share of the total number of news articles. The search is organized into eight categories: War Threats, Peace Threats, Military Buildups, Nuclear Threats, Terror Threats, Beginning of War, Escalation of War, and Terror Acts. We use the historical index, which started in 1900 and is based on three major U.S. newspapers: the Chicago Tribune, the New York Times, and the Washington Post. The bloc indicators are the weighted average of country-specific indices for each bloc with PPP GDP weights. Country-specific indices are constructed by counting the monthly share of all newspaper articles that both (1) meet the criteria for inclusion in the GPR index and (2) mention

the name of the country or its major cities. They are available for 44 different advanced and emerging countries. The resulting indices capture the U.S. perspective on risks posed by, or involving, the country in question.

Frequency. Monthly data are converted to quarterly series.

Source. Caldara and Iacoviello (2022). The extended series is available on the website. PPP GDP is obtained from the WEO Database.

13. **The energy-related uncertainty index**

Description. The energy-related uncertainty index (EUI) is constructed by text analysis of the monthly country report of the Economist Intelligence Unit for 28 developed and developing countries. An economic uncertainty index is constructed for each country following the approach in the World Uncertainty Index by Ahir et al. (2022), i.e., by counting the frequency of terms such as "uncertainty" as a share of total words in the same report. Then, the same approach is taken to calculate an energy-related index from the same source by focusing on keywords, including "energy," "oil," "OPEC," and "climate change." A global index is a simple average of countries' indices or weighted by GDP. We use the GDP-weighted index. As country-specific series are not published, we cannot create bloc indices.

Frequency. Monthly data are converted to quarterly series.

Source. Dang et al. (2023). The series is downloaded from the website.

14. **The number of international conflicts**

Description. In the Uppsala Conflict Data Program (UCDP) database, armed conflicts are incidences of the use of armed force by an organized actor against another organized actor or against civilians that result in at least one direct death. International conflicts are defined as armed conflicts across states or internationalized intra-state conflicts. As the UCDP database records the start and end of each conflict, we calculate the global indicator by counting the number of international conflicts in place each month. Bloc indicators are not constructed because the incidences of conflicts are concentrated in the Others bloc and the U.S.-EU and the China-Russia blocs do not show meaningful dynamics.

Frequency. Monthly data are converted to quarterly series.

Source. The data are taken from the UCDP Onset Dataset version 23.1 available on the website.

15. **The number of sanctions**

Description. The number of sanctions is taken from the Global Sanctions Data Base (GSDB) constructed by Felbermayr et al. (2020). The GSDB defines sanctions as binding restrictive measures applied by individual nations, country groups, the United

Nations (UN), and other international organizations to address different types of violations of international norms by inducing target countries to change their behavior or to constrain their actions. The database focuses on effective sanctions while excluding threats. The GSDB classifies sanctions by type into five categories covering trade (e.g., export/import ban), financial activity (e.g., freezing a bank account), arms (e.g., restrictions on arms sales), military assistance (e.g., prohibiting monetary or personal assistance), and travel (e.g., travel ban), plus a residual category collecting other sanctions. If a sanction spans multiple categories, it is regarded as one action. The database version 3, published in June 2023, includes 1,325 sanctions that were enforced over the 1949-2023 period. The global indicator is the total number of sanctions in place at each time point. The bloc indicators are the sum of those imposed by countries in the bloc or imposed on them. When a sanction is implemented by a group of countries or an international organization, it is counted in a bloc if at least one country joins the sanction. For instance, a sanction imposed by the UN is counted in each of the U.S.-EU, CHN-RUS, and Others blocs.

Frequency. Annual.

Source. Felbermayr et al. (2020). The extended series is available on the website.

16. **The UN General Assembly Kappa Score**

Description. The measure represents similarities in voting patterns in the United Nations General Assembly. Compared to a simple measure of the sum of the squared actual deviation between their votes (scaled by the sum of the squared maximum possible deviations between their votes), the kappa score corrects the observed variability of the countries' bilateral voting outcomes with the variability of each country's voting outcomes around its own average outcome and the difference between the two countries' average outcomes. The global indicator is the simple average of all country pairs. Bloc indicators are calculated as the simple average score of each bloc's countries.

Frequency. Annual.

Source. The data are downloaded from the database built by Häge (2017).

A.2 Sample countries

Table A-1: List of countries for the LP

Category	Countries
AEs (36 countries and territory)	Australia, Austria, Belgium, Canada, Switzerland, Cyprus, Czech, Germany, Denmark, Spain, Estonia, Finland, France, U.K., Greece, Hong Kong, Iceland, Ireland, Israel, Italy, Japan, Korea, Lithuania, Luxembourg, Latvia, Macao, Malta, Netherlands, Norway, New Zealand, Portugal, Singapore, Slovakia, Slovenia, Sweden, U.S.
EMs (53 countries and territory)	Albania, Argentina, Bulgaria, Bahamas, Bosnia and Herzegovina, Belarus, Bolivia, Brazil, Brunei, Botswana Chile, China, Colombia, Capo Verde, Costa Rica, Dominican Republic, Ecuador, Georgia, Guatemala, Croatia, Hungary, India, Indonesia, Jamaica, Jordan, Kazakhstan, Saint Lucia, Sri Lanka, Mexico, Mongolia, Montenegro, Mauritiuos, Malaysia, Namibia, North Macedonia, Paraguay, Peru, Philippines, Poland, Romania, Russia, Saudi Arabia, El Salvador, Serbia, Seychelles, Trinidad and Tobago, Thailand, Türkiye, Ukraine, Urguay, Saint Vincent and the Grenadines, West Bank and Gaza, Samoa, South Africa

Notes: Country classification of AEs and EMs follows the IMF WEO. Underlined countries have data available for the panel VAR analysis.

A.3 Descriptive statistics

Table A-2: Descriptive statistics of countries

Variable	N. of observations	Mean	Median	Std. Dev.	10th percentile	90th percentile
All countries						
GDP per capita (1,000 PPP$)	7,194	2.98	26.3	21.1	8.6	53.2
GDP growth per capita (%)	7,302	2.5	2.3	6.8	-4.0	8.6
AEs						
GDP per capita (1,000 PPP$)	3,739	44.1	40.8	19.4	26.8	61.2
GDP growth per capita (%)	3,892	2.1	2.0	5.6	-2.7	7.4
EMs						
GDP per capita (1,000 PPP$)	3,455	14.3	12.8	7.6	6.3	24.4
GDP growth per capita (%)	3,410	2.5	2.9	7.9	-5.5	9.7

Notes: Pooled sample during 1986 to 2019.

A.4 Narrative episodes

Table A-3: Fragmentation and globalization episodes

	Period	Event	Descriptions	Impact (1 for fragmentation and -1 for globalization)
1	1988:Q2	Geneva Accords between Afghanistan and Pakistan	On April 14, 1988, agreements were signed between Afghanistan and Pakistan on the settlement of the situation relating to Afghanistan at the Geneva headquarters of the United Nations, with the United States and the Soviet Union serving as guarantors.	-1
2	1988:Q4	First state sovereignty in the USSR	On November 16, 1988, Estonia was the first Soviet republic to declare state sovereignty. The event is often characterized as a trigger of the dissolution of the USSR.	-1
3	1989:Q4	Fall of the Berlin Wall	On November 9, 1989, following a press conference led by Günter Schabowski, the party leader in East Berlin and the top government spokesman, East Germans began gathering at the Berlin Wall and finally let the checkpoints open.	-1
4	1990:Q1	First independence from the USSR	On March 11, 1990, Lithuania became the first republic that declared full independence restored from the Soviet Union. This was followed by other republics' independence.	-1
5	1990:Q3	Iraqi invasion of Kuwait	On August 2, Iraq launched an invasion of Kuwait. After defeating Kuwait on August 4, Iraq went on to militarily occupy the country.	1
6	1991:Q1	Gulf War	On January 16, 1991, the U.S.-led multinational coalition started an aerial bombing campaign. The attack followed the no response by Iraq to the UNSC Resolution 678, adopted on November 29, 1990, and due by January 15, 1991, that required Iraq to withdraw from Kuwait.	1
7	1991:Q3	USSR 1991 August coup	During August 19-22, 1991, top military and civilian officials of the USSR attempted a coup to seize control of the country from Mikhail Gorbachev. Though the coup failed, it reduced the power of Gorbachev's regime and accelerated the resolution of the USSR.	-1
8	1991:Q4	Dissolution of the USSR	On December 8, 1991, Boris Yeltsin, Leonid Kravchuk, and Stanislav Shushkevich—the leaders of Russia, Ukraine, and Belarus—signed the Belovezha Accords, which declared that the Soviet Union had ceased to exist and established the Commonwealth of Independent States (CIS).	-1

Table A-4: Fragmentation and globalization episodes (cont.)

	Period	Event	Descriptions	Impact (1 for fragmentation and -1 for globalization)
8	1991:Q4	Dissolution of the USSR	On December 8, 1991, Boris Yeltsin, Leonid Kravchuk, and Stanislav Shushkevich—the leaders of Russia, Ukraine, and Belarus—signed the Belovezha Accords, which declared that the Soviet Union had ceased to exist and established the Commonwealth of Independent States (CIS).	-1
9	1994:Q1	NAFTA implementation	On January 1, 1994, the North American Free Trade Agreement (NAFTA) came into force among the U.S., Canada, and Mexico, superseding the 1988 Canada-U.S. FTA.	-1
10	1994:Q2	NATO intervention in Serbia	On April 10, 1994, NATO launched an air support mission bombing several Serb targets at the request of UN commanders, followed by the increases in NATO involvement in Bosnia.	1
11	1995:Q1	WTO formation / Mercosur implementation	On January 1, 1995, the World Trade Organization (WTO) commenced operations, replacing the General Agreement on Tariffs and Trade (GATT). As of January 1, 1995, Mercosur, a South American trade area, became a customs union with common external tariffs.	-1
12	1995:Q3	U.S.-Vietnam normalization of diplomatic relations	On July 11, 1995, U.S. President Clinton announced the normalization of relations with Vietnam, followed by the opening of each country's liaison offices later the year.	-1
13	1999:Q1	Introduction of the Euro	On January 1, 1999, the euro was introduced in non-physical form, with the irrevocable conversion rates for the euro for each participating currency set by the "joint communiqué on the determination of the irrevocable conversion rates for the euro" of May 2, 1998.	-1
14	1999:Q1	NATO intervention in Kosovo	On March 24, 1999, NATO started the bombing campaign against Yugoslavia during the Kosovo War.	-1
15	2001:Q3	9.11	On September 11, 2001, coordinated Islamist suicide terrorist attacks were carried out by Al-Qaeda against the U.S.	1
16	2003:Q1	Iraq War	On March 20, 2003, the U.S., joined by the UK, Australia, and Poland, launched a bombing campaign, followed by a ground invasion of Iraq.	1

Table A-5: Fragmentation and globalization episodes (cont.)

	Period	Event	Descriptions	Impact (1 for fragmentation and -1 for globalization)
17	2004:Q2	Expansion of EU	On April 1, 2004, the EU expanded with 10 new member states, including former USSR countries.	-1
18	2010:Q4	Arab Spring	Protests in Tunisia escalated after the self-immolation of Tunisian Mohamed Bouazizi on December 17, 2010, which led to democratization in Tunisia (Jasmine Revolution) and spread across the Arab world (Arab Spring).	1
19	2014:Q3	U.S. attack on ISIL	On August 8, 2014, the U.S. began airstrikes against the Islamic State of Iraq and the Levant (ISIL) in Iraq. This followed the declaration by the group to rename itself as an Islamic State and a worldwide caliphate on June 29, 2014.	1
20	2016:Q2	Brexit vote	On June 23, 2016, the "Brexit" referendum, which asked the electorate whether the country should remain a member of, or leave, the European Union (EU), took place in the UK. The referendum resulted in favor of leaving the EU, triggering the process of the country's withdrawal from the EU (Brexit).	1
21	2018:Q3	U.S.-China trade war (phases 1-3)	On July 6, 2018, U.S. tariffs on $34 billion of Chinese goods (announced on June 16) came into effect (phase 1). On August 23, tariffs of 25% on additional Chinese products worth $16 billion (announced on August 8) became effective (phase 2). On September 24, a 10% tariff on $200 billion worth of Chinese goods began (announced on September 17) (phase 3).	1
22	2019:Q2	U.S.-China trade war (increase in phase 3)	On May 10, 2019, the U.S. raised the tariff on phase 3 products from 10% to 25% (announced on May 5).	1
23	2019:Q3	U.S.-China trade war (phase 4)	On September 1, 2019, the U.S. imposed new 15% tariffs on about $112 billion of Chinese products.	1
24	2022:Q1	Russian invasion of Ukraine	On February 24, 2022, Russia invaded Ukraine. The invasion became the largest attack on a European country since World War II.	1

A.5 Country classification and indicators for local indices

We consider three geopolitical blocs: the U.S. and EU countries bloc (U.S.-EU), China and Russia bloc (CHN-RUS), and the remaining countries bloc (Others). EU countries are the member states of the European Union each period. The union republics of the Union of Soviet Socialist Republics (USSR) are included in the CHN-RUS bloc before its dissolution in 1991Q4. Table A-6 lists the countries, and Figure A-1 presents the fragmentation indicators for individual blocs.

Table A-6: List of countries in each bloc

Category	Countries
U.S.-EU bloc	U.S., Belgium, France, Germany, Italy, Luxembourg, Netherlands (founders); Denmark, Ireland (1973Q1-); Greece (1981Q1-); Spain (1986Q1-); Austria, Finland, Sweden (1995Q1-); Portugal (1996Q1-); Cyprus, Czechia, Estonia, Hungary, Latvia, Lithuania, Malta, Poland, Slovakia, Slovenia (2004Q2-); Bulgaria, Romania (2007Q1-); Croatia (2013Q3-); UK (-2019Q4)
CHN-RUS bloc	China, Russia, Ukrainian SSR (Ukraine), Byelorussian SSR (Belarus), Uzbek SSR (Uzbekistan), Kazakh SSR (Kazakhstan), Georgian SSR (Georgia), Azerbaijan SSR (Azerbaijan), Lithuanian SSR (Lithuania), Moldavian SSR (Moldova), Latvian SSR (Latvia), Kirghiz SSR (Kyrgyz), Tajik SSR (Tajikistan), Armenian SSR (Armenia), Turkmen SSR (Turkmenistan), Estonian SSR (Estonia) (-1991Q4)
Others bloc	All other countries

Figure A-1: Bloc indicators

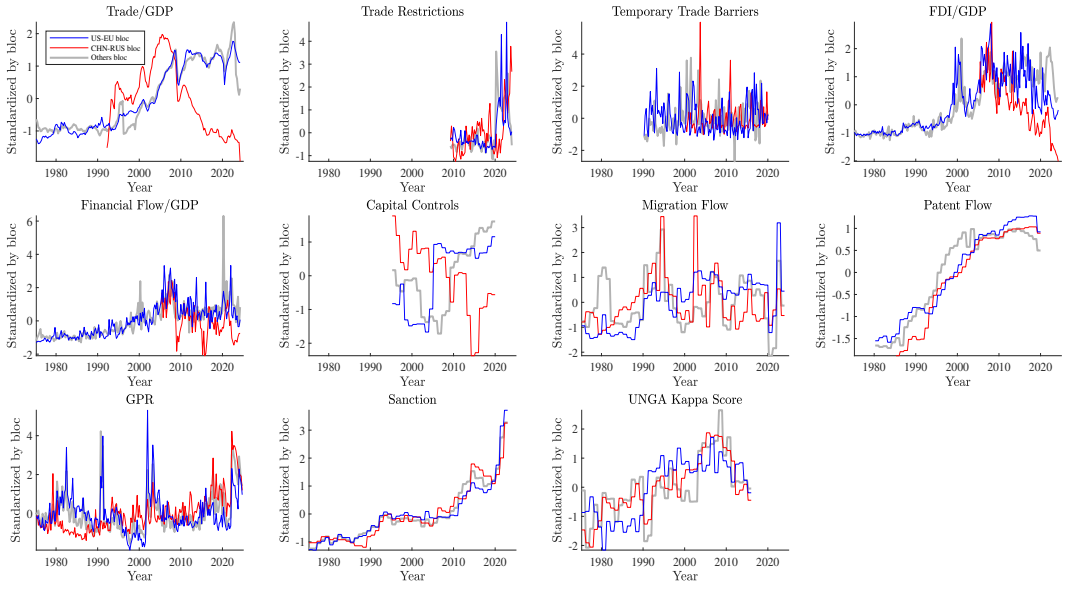

B Estimating the Dynamic Hierarchical Factor Model

The dynamic hierarchical factor model with time-varying parameters is specified as follows:

$$
\begin{aligned}
y_{k,t}^{(j)} &= a_{k,t}^{(j)} + b_{k,t}^{(j)} f_t^{(j)} + u_{k,t}^{(j)}, \\
a_{k,t}^{(j)} &= a_{k,0}^{(j)} + a_{k,1}^{(j)} t, \\
b_{k,t}^{(j)} &= b_{k,t-1}^{(j)} + \sigma_{b_k}^{(j)} \epsilon_{b_k,t}^{(j)}, \quad \epsilon_{b_k,t}^{(j)} \sim \mathcal{N}(0,1), \\
f_t^{(j)} &= f_{t-1}^{(j)} + \lambda^{(j)} \sigma_{f,t} \epsilon_{f,t} + \sigma_{f,t}^{(j)} \epsilon_{f,t}^{(j)}, \quad \epsilon_{f,t} \sim \mathcal{N}(0,1), \quad \epsilon_{f,t}^{(j)} \sim \mathcal{N}(0,1), \\
u_{k,t}^{(j)} &= \rho_{u_k,1}^{(j)} u_{k,t-1}^{(j)} + ... + \rho_{u_k,q}^{(j)} u_{k,t-q}^{(j)} + \sigma_{u_k,t}^{(j)} \epsilon_{u_k,t}^{(j)}, \quad \epsilon_{u_k,t}^{(j)} \sim \mathcal{N}(0,1), \\
\sigma_{g,t}^{(j)} &= \sigma_g^{(j)} \exp(h_{g,t}^{(j)}), \quad h_{g,t}^{(j)} = h_{g,t-1}^{(j)} + \sigma_{h_g}^{(j)} \epsilon_{h_g,t}^{(j)}, \quad \epsilon_{h_g,t}^{(j)} \sim \mathcal{N}(0,1), \quad g \in \left\{ f, u_1, \ldots, u_{N_j} \right\}, \\
\sigma_{f,t} &= \sigma_f \exp(h_{f,t}), \quad h_{f,t} = h_{f,t-1} + \sigma_{h_f} \epsilon_{h_f,t}, \quad \epsilon_{h_f,t} \sim \mathcal{N}(0,1),
\end{aligned}
$$

where $k \in \{1, \ldots, N_j\}$ and $j \in \{1, \ldots, J\}$.

B.1 Parameters and latent states

The model unknowns are collected in:

$$
\begin{aligned}
F &= \{f^T, f^{(1),T}, ..., , f^{(J),T}\}, \\
\Theta_f &= \{\sigma_f^2, \sigma_{(1),f}^2, ..., , \sigma_{(J),f}^2, \lambda^{(1)}, ..., \lambda^{(J)}\}, \\
H_f &= \{H_f^T, H_f^{(1),T}, ..., H_f^{(J),T}\}, \\
B &= \{b^{(1),T}, ..., b^{(J),T}\}, \\
\Theta_y &= \{a^{(1)}, ..., a^{(J)}, \sigma_{(1),b}^2, ..., , \sigma_{(J),b}^2\}, \\
H_u &= \{H_u^{(1),T}, ..., , H_u^{(J),T}\}, \\
\Theta_u &= \{\rho_u^{(1)}, ..., \rho_u^{(J)}, \sigma_{(1),u}^2, ..., , \sigma_{(J),u}^2\}.
\end{aligned}
$$

B.2 Gibbs sampler

We use the Gibbs sampler to estimate the model unknowns. For the m-th iteration:

(G1) Appendix B.3: Run Kalman filter and smoother algorithm to update $F^{(m)}, \Theta_f^{(m)}, H_f^{(m)}$ conditional on $B^{(m-1)}, \Theta_y^{(m-1)}, H_u^{(m-1)}, \Theta_u^{(m-1)}$.

(G2) Appendix B.4: Run Kalman filter and smoother using the algorithm to update $B^{(m)}, \Theta_y^{(m)}$ conditional on $F^{(m)}, \Theta_f^{(m)}, H_f^{(m)}, H_u^{(m-1)}, \Theta_u^{(m-1)}$.

(G3) Appendix B.5: Update the remaining parameters, $H_u^{(m)}, \Theta_u^{(m)}$ conditional on $F^{(m)}, \Theta_f^{(m)}, H_f^{(m)}$ and $B^{(m)}, \Theta_y^{(m)}$.

For ease of exposition, we omit the superscript (m) when describing the procedure below.

B.3 Updating factors F, parameters Θ_f, stochastic volatilities H_f

We define:

$$\begin{aligned}
\tilde{y}_{k,t}^{(j)} &= y_{k,t}^{(j)} - \rho_{u,k}^{(j)} y_{k,t-1}^{(j)}, \\
\tilde{a}_{k,t}^{(j)} &= a_{k,0}^{(j)}(1-\rho_{u,k}^{(j)}) + a_{k,1}^{(j)}(t - \rho_{u,k}^{(j)}(t-1)), \\
\tilde{b}_{k,t}^{(j)} &= \left[\begin{array}{cc} b_{k,t}^{(j)}, & -b_{k,t-1}^{(j)}\rho_{u,k}^{(j)} \end{array} \right],
\end{aligned}$$

and stack them in vectors

$$\tilde{y}_t^{(j)} = \left[\begin{array}{c} \tilde{y}_{1,t}^{(j)} \\ \vdots \\ \tilde{y}_{n_j,t}^{(j)} \end{array} \right], \quad \tilde{a}_t^{(j)} = \left[\begin{array}{c} \tilde{a}_{1,t}^{(j)} \\ \vdots \\ \tilde{a}_{n_j,t}^{(j)} \end{array} \right], \quad \tilde{b}_t^{(j)} = \left[\begin{array}{c} \tilde{b}_{1,t}^{(j)} \\ \vdots \\ \tilde{b}_{n_j,t}^{(j)} \end{array} \right], \quad \epsilon_{u,t}^{(j)} = \left[\begin{array}{c} \epsilon_{u_1,t}^{(j)} \\ \vdots \\ \epsilon_{u_{n_j},t}^{(j)} \end{array} \right],$$

$$var(\epsilon_{u,t}^{(j)}) = \text{BlockDiagonal} \left[\begin{array}{c} \sigma_{(j),u_1}^2 \exp(2h_{u_1,t}^{(j)}) \\ \vdots \\ \sigma_{(j),u_{n_j}}^2 \exp(2h_{u_{n_j},t}^{(j)}) \end{array} \right], \quad var(\epsilon_{f,t}^{(j)}) = \sigma_{(j),f}^2 \exp(2h_{f,t}^{(j)}).$$

Then, we have the following state-space representation:

$$\left[\begin{array}{c} \tilde{y}_t^{(1)} \\ \vdots \\ \tilde{y}_t^{(J)} \end{array} \right] = \left[\begin{array}{c} \tilde{a}_t^{(1)} \\ \vdots \\ \tilde{a}_t^{(J)} \end{array} \right] + \text{BlockDiagonal}\left(\begin{array}{cccc} 0 & \tilde{b}_t^{(1)} & \ldots & \tilde{b}_t^{(J)} \end{array} \right) \cdot s_t + \left[\begin{array}{c} \epsilon_{u,t}^{(1)} \\ \vdots \\ \epsilon_{u,t}^{(J)} \end{array} \right],$$

$$\underbrace{\left[\begin{array}{c} f_t \\ f_t^{(1)} \\ f_{t-1}^{(1)} \\ \vdots \\ f_t^{(J)} \\ f_{t-1}^{(J)} \end{array} \right]}_{s_t} = \left[\begin{array}{cccccc} 1 & 0 & 0 & \ldots & 0 & 0 \\ 0 & 1 & 0 & \ldots & 0 & 0 \\ 0 & 1 & 0 & \ldots & 0 & 0 \\ \vdots & \vdots & \vdots & \ddots & \vdots & \vdots \\ 0 & 0 & 0 & \ldots & 1 & 0 \\ 0 & 0 & 0 & \ldots & 1 & 0 \end{array} \right] \left[\begin{array}{c} f_{t-1} \\ f_{t-1}^{(1)} \\ f_{t-2}^{(1)} \\ \vdots \\ f_{t-1}^{(J)} \\ f_{t-2}^{(J)} \end{array} \right] + \left[\begin{array}{cccc} 1 & 0 & \ldots & 0 \\ \lambda^{(1)} & 1 & \ldots & 0 \\ 0 & 0 & \ldots & 0 \\ \vdots & \vdots & \ddots & \vdots \\ \lambda^{(J)} & 0 & \ldots & 1 \\ 0 & 0 & \ldots & 0 \end{array} \right] \left[\begin{array}{c} \epsilon_{f,t} \\ \epsilon_{f,t}^{(1)} \\ \vdots \\ \epsilon_{f,t}^{(J)} \end{array} \right].$$

and we obtain smoothed estimates of F.

We construct:

$$z_t^{(j)} = \frac{f_t^{(j)} - f_{t-1}^{(j)}}{\exp(h_{f,t}^{(j)})}, \quad x_t^{(j)} = \frac{f_t - f_{t-1}}{\exp(h_{f,t}^{(j)})},$$

from which we can update the loading $\lambda^{(j)}$ on $x_t^{(j)}$ in explaining $z_t^{(j)}$ and the residual variance $\sigma_{(j),f}^2$. Similarly, we construct $z_t = \frac{f_t - f_{t-1}}{\exp(h_{f,t})}$ to update σ_f^2.

Define:

$$\gamma_t = \frac{f_t - f_{t-1}}{\sigma_f}, \quad \gamma_t^{(j)} = \frac{f_t^{(j)} - f_{t-1}^{(j)} - \lambda^{(j)}(f_t - f_{t-1})}{\sigma_{(j),f}}$$

to update H_f. The detailed procedures for these steps are provided in Appendix B.6 and Appendix B.7.

B.4 Updating factor loadings B and parameters Θ_y

We define:

$$\begin{aligned}
\tilde{y}_{k,t}^{(j)} &= y_{k,t}^{(j)} - \rho_{u,k}^{(j)} y_{k,t-1}^{(j)}, \\
\tilde{a}_{k,t}^{(j)} &= a_{k,0}^{(j)}(1 - \rho_{u,k}^{(j)}) + a_{k,1}^{(j)}(t - \rho_{u,k}^{(j)}(t-1)), \\
\tilde{f}_{k,t}^{(j)} &= \left[\begin{array}{cc} f_t^{(j)}, & -f_{t-1}^{(j)} \rho_{u,k}^{(j)} \end{array} \right].
\end{aligned}$$

Then, we have the following state-space representation:

$$\begin{aligned}
\left[\begin{array}{c} \tilde{y}_{1,t}^{(j)} \\ \vdots \\ \tilde{y}_{n_j,t}^{(j)} \end{array} \right] &= \left[\begin{array}{c} \tilde{a}_{1,t}^{(j)} \\ \vdots \\ \tilde{a}_{n_j,t}^{(j)} \end{array} \right] + \text{BlockDiagonal}\left(\begin{array}{ccc} \tilde{f}_{1,t}^{(j)} & \dots & \tilde{f}_{n_j,t}^{(j)} \end{array} \right) \cdot s_t + \left[\begin{array}{c} \epsilon_{u_1,t}^{(j)} \\ \vdots \\ \epsilon_{u_{n_j},t}^{(j)} \end{array} \right], \\
\underbrace{\left[\begin{array}{c} b_{1,t}^{(j)} \\ b_{1,t-1}^{(j)} \\ \vdots \\ b_{n_j,t}^{(j)} \\ b_{n_j,t-1}^{(j)} \end{array} \right]}_{s_t} &= \left[\begin{array}{ccccc} 1 & 0 & \dots & 0 & 0 \\ 1 & 0 & \dots & 0 & 0 \\ \vdots & \vdots & \ddots & \vdots & \vdots \\ 0 & 0 & \dots & 1 & 0 \\ 0 & 0 & \dots & 1 & 0 \end{array} \right] \left[\begin{array}{c} b_{1,t-1}^{(j)} \\ b_{1,t-2}^{(j)} \\ \vdots \\ b_{n_j,t-1}^{(j)} \\ b_{n_j,t-2}^{(j)} \end{array} \right] + \left[\begin{array}{ccc} 1 & \dots & 0 \\ 0 & \dots & 0 \\ \vdots & \ddots & \vdots \\ 0 & \dots & 1 \\ 0 & \dots & 0 \end{array} \right] \left[\begin{array}{c} \epsilon_{b_1,t}^{(j)} \\ \vdots \\ \epsilon_{b_{n_j},t}^{(j)} \end{array} \right].
\end{aligned}$$

Conditional on B, we can construct $z_{k,t}^{(j)} = b_{k,t}^{(j)} - b_{k,t-1}^{(j)}$ to update $\sigma_{(j),b_k}^2$.

We define:

$$\begin{aligned}
z_{k,t}^{(j)} &= \frac{y_{k,t}^{(j)} - \rho_{u,k}^{(j)} y_{k,t-1}^{(j)} - \left[\begin{array}{cc} b_{k,t}^{(j)}, & -b_{k,t-1}^{(j)} \rho_{u,k}^{(j)} \end{array} \right] \left[\begin{array}{c} f_t^{(j)} \\ f_{t-1}^{(j)} \end{array} \right]}{\exp(h_{u_k}^{(j)})}, \\
x_{k,t}^{(j)} &= \left[\begin{array}{cc} \frac{1-\rho_{u,k}^{(j)}}{\exp(h_{u_k}^{(j)})}, & \frac{t-\rho_{u,k}^{(j)}(t-1)}{\exp(h_{u_k}^{(j)})} \end{array} \right],
\end{aligned}$$

and update the loading on $x_{k,t}^{(j)}$ in explaining $z_{k,t}^{(j)}$ which is $[a_{k,0}^{(j)}, a_{k,1}^{(j)}]'$. We repeat this for each $j \in \{1, ..., J\}$ and $k \in \{1, ..., n_j\}$.

The detailed procedures are provided in Appendix B.6 and Appendix B.7.

B.5 Updating parameters Θ_u and stochastic volatilities H_u

We construct:

$$z_{k,t}^{(j)} = \frac{\tilde{z}_{k,t}^{(j)}}{\exp(h_{u_k}^{(j)})}, \quad \tilde{z}_{k,t}^{(j)} = y_{k,t}^{(j)} - a_{k,t}^{(j)} - b_{k,t}^{(j)} f_t^{(j)}, \quad x_{k,t}^{(j)} = \frac{\tilde{z}_{k,t-1}^{(j)}}{\exp(h_{u_k}^{(j)})}$$

to update the loading $\rho_{u_k}^{(j)}$ on $x_{k,t}^{(j)}$ in explaining $z_{k,t}^{(j)}$ and the residual variance $\sigma_{(j),u_k}^2$.

Also, we construct:

$$z_{k,t}^{(j)} = \frac{\tilde{z}_{k,t}^{(j)} - \rho_{u_k}^{(j)} \tilde{z}_{k,t-1}^{(j)}}{\sigma_{(j),u_k}}, \quad \tilde{z}_{k,t}^{(j)} = y_{k,t}^{(j)} - a_{k,t}^{(j)} - b_{k,t}^{(j)} f_t^{(j)},$$

to update $h_{u_k}^{(j),T}$. We repeat this for each $j \in \{1, ..., J\}$ and $k \in \{1, ..., n_j\}$.

The detailed procedures are provided in Appendix B.7.

B.6 Forward filtering and backward smoothing algorithm

To illustrate the forward filtering and backward smoothing algorithm by Carter and Kohn (1994), we will use a generic expression for the state-space model:

$$\begin{aligned} o_t &= A + Z_t s_t + \eta_t, \quad \eta_t \sim \mathcal{N}(0, \Omega_t), \\ s_t &= \Phi s_{t-1} + \varepsilon_t, \quad \varepsilon_t \sim \mathcal{N}(0, \Sigma_t). \end{aligned}$$

We summarize the Kalman filter as described in Durbin and Koopman (2001). Suppose that $s_{t-1}|y^{t-1} \sim \mathcal{N}(s_{t-1|t-1}, P_{t-1|t-1})$. Then, the Kalman forecasting and updating equations are:

$$\begin{aligned} s_{t|t-1} &= \Phi s_{t-1|t-1} \\ P_{t|t-1} &= \Phi P_{t-1|t-1} \Phi' + \Sigma_t \\ s_{t|t} &= s_{t|t-1} + (Z_t P_{t|t-1})' (Z_t P_{t|t-1} Z_t')^{-1} \left(o_t - A - Z_t s_{t|t-1}\right) \\ P_{t|t} &= P_{t|t-1} - (Z_t P_{t|t-1})' (Z_t P_{t|t-1} Z_t')^{-1} (Z_t P_{t|t-1}). \end{aligned}$$

In turn, $s_t|o^t \sim \mathcal{N}(s_{t|t}, P_{t|t})$.

The backward smoothing algorithm developed by Carter and Kohn (1994) is applied to generate draws from the distributions $s_\tau$recursively$|s_{\tau+1}, ..., s_T, o^T$ (ignoring dependency on model unknowns) for $\tau = T-1, T-2, \ldots, 1$. The last elements of the Kalman filter recursion

provide the initialization for the simulation smoother:

$$
\begin{aligned}
s_{\tau|\tau+1} &= s_{\tau|\tau} + P_{\tau|\tau}\Phi' P^{-1}_{\tau+1|t}\left(s_{\tau+1} - \Phi s_{\tau|\tau}\right) \\
P_{\tau|\tau+1} &= P_{\tau|\tau} - P_{\tau|\tau}\Phi' P^{-1}_{\tau+1|\tau}\Phi P_{\tau|\tau} \\
\text{draw } s_\tau &\sim N(s_{\tau|\tau+1}, P_{\tau|\tau+1}), \qquad \tau = T-1, T-2, ..., 1.
\end{aligned}
$$

B.7 Drawing persistence, variance, and stochastic volatility of the autoregressive model

To illustrate the procedure, we explain how to draw the persistence, variance, and stochastic volatility with a simple AR(1) model:

$$x_t = \rho_x x_{t-1} + \sigma_x \exp(h_t)\epsilon_{x,t}, \quad \epsilon_{x,t} \sim \mathcal{N}(0,1). \tag{A-1}$$

Drawing ρ_x. In order to obtain the posterior for ρ_x, we assume that for $t \leq 0$, $h_t = 0$. Under this assumption, x_0 is generated from a stationary distribution. Express the unconditional distribution as $x_0 \sim \mathcal{N}(0, \Sigma_{x_0})$, where $\Sigma_{x_0} = \frac{1}{(1-\rho_x^2)}$. From equation (A-1), we get $var(x_1) = \rho_x^2 var(x_0) + \exp(2h_1) = S_{x_0}$, where $S_{x_0} = \rho_x^2 \Sigma_{x_0} + \exp(2h_1)$.

We write the conditional likelihood of the first-factor element as:

$$\mathcal{L}(x_1|h_1, \rho_x) = \frac{1}{\sqrt{2\pi S_{x0}}} \exp\left\{-\frac{1}{2S_{x0}} x_1^2\right\},$$

and the remaining $T-1$ elements as:

$$
\begin{aligned}
\mathcal{L}(x_2, ..., x_T|h_{1:T}, \rho_x) &= \prod_{t=2}^{T} \frac{1}{\sqrt{2\pi \exp(2h_t)}} \exp\left\{-\frac{1}{2}\left(\frac{x_t - \rho_x x_{t-1}}{\exp(h_t)}\right)'\left(\frac{x_t - \rho_x x_{t-1}}{\exp(h_t)}\right)\right\} \\
&\propto \exp\left\{\frac{1}{2}(e_0 - E_0\rho_x)'(e_0 - E_0\rho_x)\right\}
\end{aligned}
$$

where:

$$e_0 = \begin{bmatrix} \frac{x_2}{\exp(h_2)} \\ \vdots \\ \frac{x_T}{\exp(h_T)} \end{bmatrix}, \quad E_0 = \begin{bmatrix} \frac{x_1}{\exp(h_2)} \\ \vdots \\ \frac{x_{T-1}}{\exp(h_T)} \end{bmatrix}.$$

We use $\rho_x \sim \mathcal{N}(V_{\rho_x}^{-1}(\bar{V}_{\rho_x}\bar{\rho}_x + E_0' e_0), V_{\rho_x}^{-1})$ as a proposal distribution, where $V_{\rho_x} = \bar{V}_{\rho_x} + E_0' E_0$. In a Metropolis-Hastings step, we accept the draw ρ_x generated from the proposal distribution with probability $\min\left\{\frac{\mathcal{L}(x_1|h_1, \rho_x^{(k)})}{\mathcal{L}(x_1|h_1, \rho_x^{(k-1)})}, 1\right\}$.

Drawing σ_x^2. The posterior for σ_x^2 is given by:

$$\sigma_x^2 \sim \mathcal{IG}\left(\frac{\bar{T}+T}{2}, \bar{v} + (e_0 - E_0\rho_x)'(e_0 - E_0\rho_x)\right).$$

Drawing h^T. The last step of the Gibbs sampler draws the stochastic volatilities conditional on all other parameters. Define γ_t such that:

$$\gamma_t = \left(\frac{x_t - \rho_x x_{t-1}}{\sigma_x}\right) = \exp(h_t)\epsilon_{x,t}.$$

Taking squares and then logs of z_t produces $z_t^* = 2h_t + u_t^*$ and $h_t = \rho_h h_{t-1} + \sigma_h \varepsilon_t$, where $z_t^* = \ln(\gamma_t^2 + 0.001)$ and $u_t^* = \ln(\epsilon_{x,t}^2)$. Observe that ε_t and u_t^* are not correlated.

The resulting state-space representation is linear but not Gaussian since the measurement error u_t^* is distributed as a $\ln(\chi_1^2)$. We approximate $\ln(\chi_1^2)$ using a mixture of normals and transform the system into a Gaussian one following Kim et al. (1998). Express the distribution of u_t^* as:

$$f(u_t^*) = \sum_{k=1}^{K} q_k f_N(u_t^* | \iota_t = k),$$

where ι_t is the indicator variable selecting which member of the mixture of normals has to be used at time t. The function $f_N(\cdot)$ denotes the pdf of a normal distribution, and $q_k = \Pr(\iota_t = k)$. Kim et al. (1998) select a mixture of seven normals ($K = 7$) with component probabilities q_k, means $m_k - 1.2704$, and variances r_k^2 (see Table A-7 below).

Table A-7: Approximating constants: $\{q_k, m_k, r_k\}$

ι	$q_k = Pr(\iota = k)$	m_k	r_k^2
1	0.00730	-10.12999	5.79596
2	0.10556	-3.97281	2.61369
3	0.00002	-8.56686	5.17950
4	0.04395	2.77786	0.16735
5	0.34001	0.61942	0.64009
6	0.24566	1.79518	0.34023
7	0.25750	-1.08819	1.26261

Conditional on $\iota_{1:T}$, the system has an approximate linear and Gaussian state-space form to which the standard Kalman filtering algorithm and the backward recursion of Carter and Kohn (1994) can be applied. Drawing h^T is, then, straightforward. The parameters associated

with h^T can be generated from the posterior distributions:

$$\begin{aligned}\rho_h &\sim \mathcal{N}\left(V_{\rho_h}^{-1}(\bar{V}_{\rho_h}\bar{\rho}_h + \sigma_h^{-2}h'_{1:T-1}h_{2:T}), V_{\rho_h}^{-1}\right)\\ \sigma_h^2 &\sim \mathcal{IG}\left(\frac{\bar{T}_h + T}{2}, \bar{v}_h + d_h^2\right)\end{aligned}$$

where $V_{\rho_h} = \bar{V}_{\rho_h} + \sigma_h^{-2}h'_{1:T-1}h_{1:T-1}$ and $d_h^2 = (h_{2:T} - \rho_h h_{1:T})'(h_{2:T} - \rho_h h_{1:T})$.

The final task is to draw a new sample of indicators, $\iota_{1:T}$ conditional on u_t^* and h_t:

$$\Pr(\iota_t = k|u_t^*, h_t) \propto q_k f_N(u_{jt}^*|2h_t + m_k - 1.2704, r_k^2).$$

C Estimation of the Non-Hierarchical Model with Two Factors

The DFM with time-varying parameters is specified as follows:

$$
\begin{aligned}
y_{i,t} &= a_{i,t} + b_{i,t} f_{1,t} + c_{i,t} f_{2,t} + u_{i,t}, \\
a_{i,t} &= a_{i,0} + a_{i,1} t, \\
f_{1,t} &= \phi_{f_1,1} f_{1,t-1} + ... + \phi_{f_1,p} f_{1,t-p} + \sigma_{f_1,t} \epsilon_{f_1,t}, \quad \epsilon_{f_1,t} \sim \mathcal{N}(0,1), \\
f_{2,t} &= \phi_{f_2,1} f_{2,t-1} + ... + \phi_{f_2,p} f_{2,t-p} + \sigma_{f_2,t} \epsilon_{f_2,t}, \quad \epsilon_{f_2,t} \sim \mathcal{N}(0,1), \\
b_{i,t} &= b_{i,t-1} + \sigma_{b_i} \epsilon_{b_i,t}, \quad \epsilon_{b_i,t} \sim \mathcal{N}(0,1), \\
c_{i,t} &= c_{i,t-1} + \sigma_{c_i} \epsilon_{c_i,t}, \quad \epsilon_{c_i,t} \sim \mathcal{N}(0,1), \\
u_{i,t} &= \phi_{u_i,1} u_{i,t-1} + ... + \phi_{u_i,q} u_{i,t-q} + \sigma_{u_i,t} \epsilon_{u_i,t}, \quad \epsilon_{u_i,t} \sim \mathcal{N}(0,1), \\
h_{j,t} &= h_{j,t-1} + \sigma_{h_j} \epsilon_{h_j,t}, \quad \sigma_{j,t} = \sigma_j \exp(h_{j,t}), \quad \epsilon_{h_j,t} \sim \mathcal{N}(0,1),
\end{aligned} \tag{A-2}
$$

where $i \in \{1, ..., N\}$ and $j \in \{f_1, f_2, u_1, ..., u_N\}$. To simplify the explanation, we gather the parameters in the system (A-2) as:

$$
a_0 = \begin{bmatrix} a_{0,1} \\ \vdots \\ a_{0,N} \end{bmatrix}, \quad a_1 = \begin{bmatrix} a_{1,1} \\ \vdots \\ a_{1,N} \end{bmatrix}, \quad b_t = \begin{bmatrix} b_{1,t} \\ \vdots \\ b_{N,t} \end{bmatrix}, \quad c_t = \begin{bmatrix} c_{1,t} \\ \vdots \\ c_{N,t} \end{bmatrix},
$$

$$
\sigma_b = \begin{bmatrix} \sigma_{b_1} \\ \vdots \\ \sigma_{b_N} \end{bmatrix}, \quad \sigma_c = \begin{bmatrix} \sigma_{c_1} \\ \vdots \\ \sigma_{c_N} \end{bmatrix}, \quad \phi_{f_1} = \begin{bmatrix} \phi_{f_1,1} \\ \vdots \\ \phi_{f_1,p} \end{bmatrix}, \quad \phi_{f_2} = \begin{bmatrix} \phi_{f_2,1} \\ \vdots \\ \phi_{f_2,p} \end{bmatrix},
$$

$$
\phi_{u_i} = \begin{bmatrix} \phi_{u_i,1} \\ \vdots \\ \phi_{u_i,q} \end{bmatrix}, \quad \phi_u = \begin{bmatrix} \phi_{u_1} \\ \vdots \\ \phi_{u_N} \end{bmatrix}, \quad \sigma_u = \begin{bmatrix} \sigma_{u_1} \\ \vdots \\ \sigma_{u_N} \end{bmatrix}, \quad \sigma_{h_u} = \begin{bmatrix} \sigma_{h_{u_1}} \\ \vdots \\ \sigma_{h_{u_N}} \end{bmatrix},
$$

$$
h_u^T = \begin{bmatrix} h_{u_1,1} & \cdots & h_{u_N,1} \\ \vdots & & \vdots \\ h_{u_1,T} & \cdots & h_{u_N,T} \end{bmatrix}.
$$

The model unknowns can be categorized into three sets:

$$
\begin{aligned}
&\Theta_f = \{f_1^T, \phi_{f_1}, \sigma_{f_1}, h_{f_1}^T, \sigma_{h_{f_1}}, f_2^T, \phi_{f_2}, \sigma_{f_2}, h_{f_2}^T, \sigma_{h_{f_2}}\}, \quad \Theta_b = \{b^T, \sigma_b, c^T, \sigma_c\}, \\
&\Theta_u = \{a_0, a_1, \phi_u, \sigma_u, h_u^T, \sigma_{h_u}\}.
\end{aligned}
$$

C.1 Gibbs sampler

We use the Gibbs sampler to estimate the model unknowns. For the k-th iteration:

(G1) Appendix C.2: Run Kalman filter and smoother using the algorithm to update $\Theta_f^{(k)}$ conditional on $\Theta_f^{(k-1)}, \Theta_b^{(k-1)}, \Theta_u^{(k-1)}$.

(G2) Appendix C.3: Run Kalman filter and smoother using the algorithm to update $\Theta_b^{(k)}$ conditional on $\Theta_f^{(k)}, \Theta_b^{(k-1)}, \Theta_u^{(k-1)}$.

(G3) Appendix C.4: Update the remaining parameters, including ones associated with the serially correlated innovation $\Theta_u^{(k)}$ conditional on $\Theta_f^{(k)}, \Theta_b^{(k)}, \Theta_u^{(k-1)}$.

For ease of exposition, we omit the superscript (k) when describing the procedure below.

C.2 Updating the factor and the associated parameters Θ_f

We re-express the system (A-2) as:

$$
\begin{aligned}
\tilde{y}_{i,t} &= \tilde{a}_{i,t} + \tilde{b}_{i,t}\tilde{f}_t + \sigma_{u_i,t}\epsilon_{u_i,t}, \\
\tilde{y}_{i,t} &= (y_{i,t} - \phi_{u_i,1}y_{i,t-1}... - \phi_{u_i,q}y_{i,t-q}), \\
\tilde{a}_{i,t} &= a_{i,0}(1 - \phi_{u_i,1}... - \phi_{u_i,q}) + a_{i,1}(t - \phi_{u_i,1}(t-1)... - \phi_{u_i,q}(t-q)), \\
\tilde{b}_{i,t} &= \left[\begin{array}{cccccccc} b_{i,t} & -b_{i,t-1}\phi_{u_i,1} & \dots & -b_{i,t-q}\phi_{u_i,q} & c_{i,t} & -c_{i,t-1}\phi_{u_i,1} & \dots & -c_{i,t-q}\phi_{u_i,q} \end{array} \right], \\
\tilde{f}_t &= \left[\begin{array}{cccccccc} f_{1,t} & f_{1,t-1} & \dots & f_{1,t-q} & f_{2,t} & f_{2,t-1} & \dots & f_{2,t-q} \end{array} \right]'.
\end{aligned}
\tag{A-3}
$$

Note that the system (A-3) implies the state-space representation:

$$\begin{bmatrix} \tilde{y}_{1,t} \\ \vdots \\ \tilde{y}_{N,t} \end{bmatrix} = \begin{bmatrix} \tilde{a}_{1,t} \\ \vdots \\ \tilde{a}_{N,t} \end{bmatrix} + \begin{bmatrix} \tilde{b}_{1,t} \\ \vdots \\ \tilde{b}_{N,t} \end{bmatrix} \cdot \begin{bmatrix} f_{1,t} \\ f_{1,t-1} \\ \vdots \\ f_{1,t-q} \\ f_{2,t} \\ f_{2,t-1} \\ \vdots \\ f_{2,t-q} \end{bmatrix} + \begin{bmatrix} \sigma_{u_1,t}\epsilon_{u_1,t} \\ \vdots \\ \sigma_{u_N,t}\epsilon_{u_N,t} \end{bmatrix},$$

$$\begin{bmatrix} f_{1,t} \\ f_{1,t-1} \\ \vdots \\ f_{1,t-q} \\ f_{2,t} \\ f_{2,t-1} \\ \vdots \\ f_{2,t-q} \end{bmatrix} = \begin{bmatrix} \begin{bmatrix} \phi'_{f_1} & 0_{1\times(q+1-p)} \\ I_q & 0_{q\times 1} \end{bmatrix} & 0_{(q+1)\times(q+1)} \\ 0_{(q+1)\times(q+1)} & \begin{bmatrix} \phi'_{f_2} & 0_{1\times(q+1-p)} \\ I_q & 0_{q\times 1} \end{bmatrix} \end{bmatrix} \begin{bmatrix} f_{1,t-1} \\ f_{1,t-2} \\ \vdots \\ f_{1,t-q-1} \\ f_{2,t-1} \\ f_{2,t-2} \\ \vdots \\ f_{2,t-q-1} \end{bmatrix} + \begin{bmatrix} \sigma_{f_1,t}\epsilon_{f_1,t} \\ 0 \\ \vdots \\ 0 \\ \sigma_{f_2,t}\epsilon_{f_2,t} \\ 0 \\ \vdots \\ 0 \end{bmatrix}. \tag{A-4}$$

Based on the state-space representation (A-4), we draw f_1^T, f_2^T based on the forward filtering and backward smoothing algorithm explained in Appendix B.6. Conditional on the drawn f_i^T, where $i \in \{1, 2\}$, we draw $\{\phi_{f_i}, \sigma_{f_i}, h_{f_i}^T, \sigma_{h_{f_i}}\}$ based on the procedure described in Appendix B.7.

C.3 Updating the factor loading and the associated parameters Θ_b

For each $i \in \{1, ..., N\}$, we re-express the system (A-2) as:

$$
\begin{aligned}
\hat{y}_{i,t} &= \hat{a}_{i,t} + \hat{f}_t \hat{b}_{i,t} + \sigma_{u_i,t}\epsilon_{u_i,t}, \\
\hat{y}_{i,t} &= (y_{i,t} - \phi_{u_i,1} y_{i,t-1} ... - \phi_{u_i,q} y_{i,t-q}), \\
\hat{a}_{i,t} &= a_{i,0}(1 - \phi_{u_i,1} ... - \phi_{u_i,q}) + a_{i,1}(t - \phi_{u_i,1}(t-1) ... - \phi_{u_i,q}(t-q)), \\
\hat{f}_t &= \begin{bmatrix} f_{1,t} & -f_{1,t-1}\phi_{u_i,1} & \dots & -f_{1,t-q}\phi_{u_i,q} & f_{2,t} & -f_{2,t-1}\phi_{u_i,1} & \dots & -f_{2,t-q}\phi_{u_i,q} \end{bmatrix}, \\
\hat{b}_{i,t} &= \begin{bmatrix} b_{i,t} \\ b_{i,t-1} \\ \vdots \\ b_{i,t-q} \\ c_{i,t} \\ c_{i,t-1} \\ \vdots \\ c_{i,t-q} \end{bmatrix} = \begin{bmatrix} \begin{bmatrix} 1 & 0_{1\times q} \\ I_q & 0_{q\times 1} \end{bmatrix} & 0_{(q+1)\times(q+1)} \\ 0_{(q+1)\times(q+1)} & \begin{bmatrix} 1 & 0_{1\times q} \\ I_q & 0_{q\times 1} \end{bmatrix} \end{bmatrix} \begin{bmatrix} b_{i,t-1} \\ b_{i,t-2} \\ \vdots \\ b_{i,t-q-1} \\ c_{i,t-1} \\ c_{i,t-2} \\ \vdots \\ c_{i,t-q-1} \end{bmatrix} + \begin{bmatrix} \sigma_{b_i}\epsilon_{b_i,t} \\ 0 \\ \vdots \\ 0 \\ \sigma_{c_i}\epsilon_{c_i,t} \\ 0 \\ \vdots \\ 0 \end{bmatrix}.
\end{aligned} \tag{A-5}
$$

Based on the state-space representation (A-5), we draw $\{b_i^T, c_i^T\}$ based on the forward filtering and backward smoothing algorithm explained in Appendix B.6. Conditional on the drawn $\{b_i^T, c_i^T\}$, we draw $\{\sigma_{b_i}, \sigma_{c_i}\}$ based on the procedure described in Appendix B.7.

C.4 Updating the remaining parameters: Θ_u

We re-express the system (A-2) as:

$$\bar{y}_{i,t} = a_i \bar{x}_{i,t} + \sigma_{u_i}\epsilon_{u_i,t},$$

where:

$$\bar{y}_{i,t} = \frac{\hat{y}_{i,t} - \hat{f}_t \hat{b}_{i,t}}{\exp(h_{u_i,t})}, \quad \bar{x}_{i,t} = \begin{bmatrix} \frac{1-\phi_{u_i,1}...-\phi_{u_i,q}}{\exp(h_{u_i,t})}, & \frac{t-\phi_{u_i,1}(t-1)...-\phi_{u_i,q}(t-q)}{\exp(h_{u_i,t})} \end{bmatrix},$$

and $\hat{y}_{i,t}$, $\hat{f}_t$, and $\hat{b}_{i,t}$ are provided in representation (A-5). We draw a_i based on the procedure described in Appendix B.7. Second, conditional on the updated a, we re-express the system (A-2) as $u_{i,t} = y_{i,t} - a_{i,t} - b_{i,t}f_{1,t} - c_{i,t}f_{2,t}$ and update the associated parameters and stochastic volatilities $\{\phi_u, \sigma_u, h_u^T, \sigma_{h_u}\}$ of the serially correlated errors based on the procedure described in Appendix B.7.

D Supplementary Figures and Tables

D.1 Posterior estimates

Figure A-2: Posterior estimates: Constants, persistence, volatilities

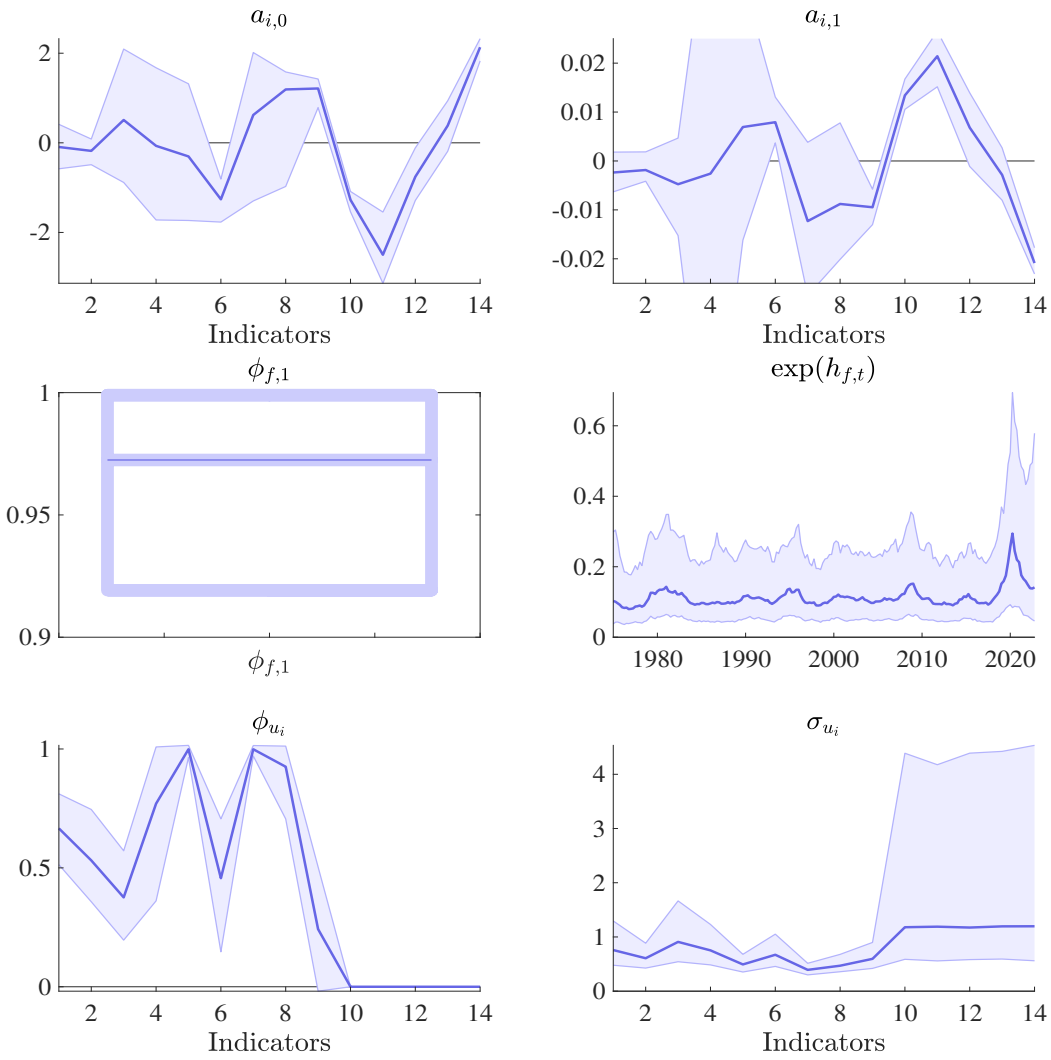

Notes: Posterior median estimates are reported with 90% credible intervals. The numerical assignment of each indicator follows the sequential order displayed in Panel (A) of Figure 1.

D.2 Robustness checks

D.2.1 Using Trade openness instead: Replicating the SVAR results

Figure A-3: Sensitivity to replacing the fragmentation index with trade openness

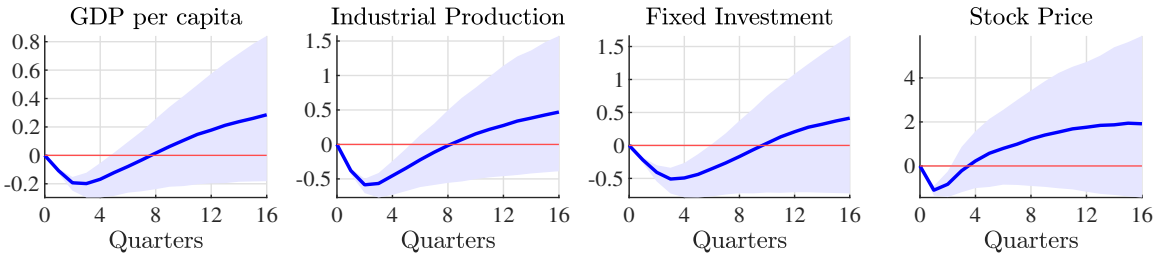

Notes: The fragmentation index is replaced with the trade share in the SVAR. Sample of AEs and EMs. Percent responses to a one-standard-deviation shock to each indicator. The sign of the responses is flipped. Shaded areas indicate the 90th percentile.

D.2.2 Alternative Cholesky ordering: Replicating the SVAR results

Figure A-4: SVAR with different Cholesky ordering

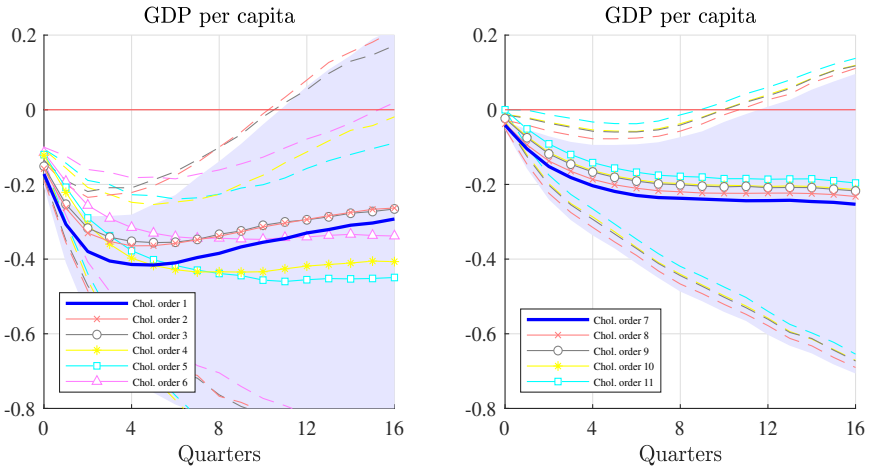

Notes: Sample of AEs and EMs. Percent responses to a one-standard-deviation fragmentation shock. Different lines display the IRFs in which the fragmentation index is ordered in the i-th place in the Cholesky decomposition. The ordering of other variables is kept unchanged. Shaded areas and dashed lines indicate the 90th percentiles where standard errors are clustered by time.

D.2.3 Alternative identification schemes: Replicating the LP results

Figure A-5: LP: Sensitivity to alternative identification schemes

(A) Identified through differencing

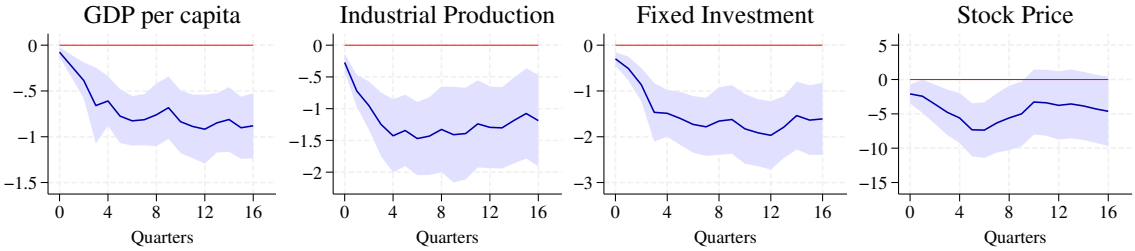

(B) Identified through Cholesky decomposition with the last ordering

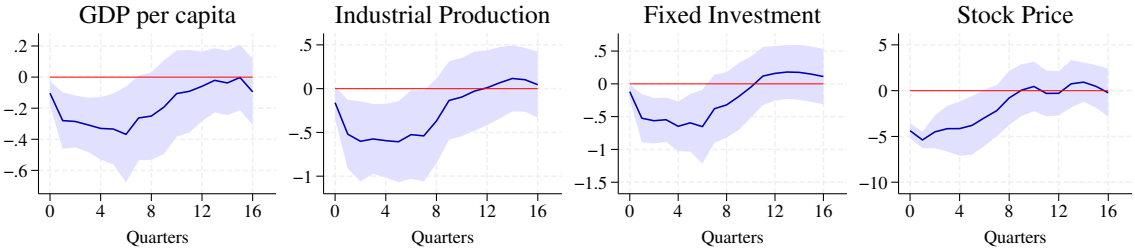

(C) Identified through regressing on military spending and monetary policy shocks

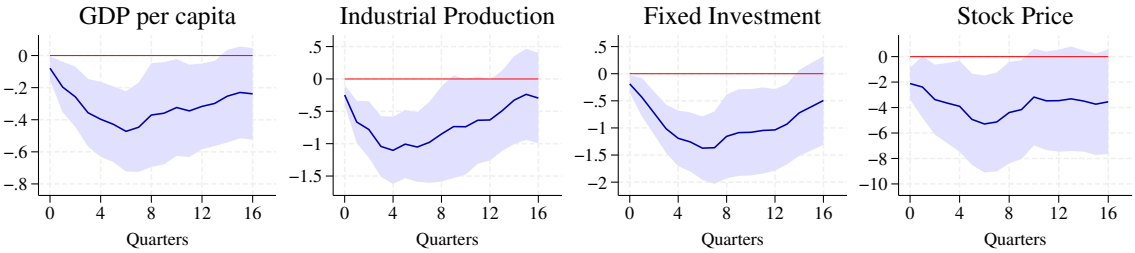

(D) Identified through narrative approach

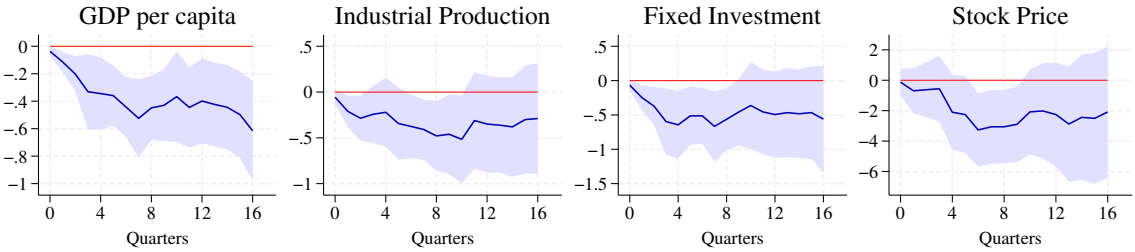

Notes: Sample of AEs and EMs. Percent responses to a one-standard-deviation shock to the factor. Shaded areas indicate the 90th percentile. In Panel (A), the first difference of the factor is used as a shock. In Panel (B), the fragmentation shock is identified through the Cholesky decomposition in the panel VAR, with the fragmentation index placed at the last of the variables. In Panel (C), the Cholesky decomposition shock is regressed on the military news shock by Ramey (2011) (updated series obtained from Ramey, 2016) and the monetary policy shock of Jarociński and Karadi (2020), and the residuals are used as shocks. In Panel (D), the reduced-form SVAR shocks are regressed on narrative shocks.

D.2.4 Alternative identification assumption of zero and sign restrictions: SVAR

Figure A-6: Economic impact of group-specific fragmentation: SVAR with zero/sign restrictions under alternative identification assumption

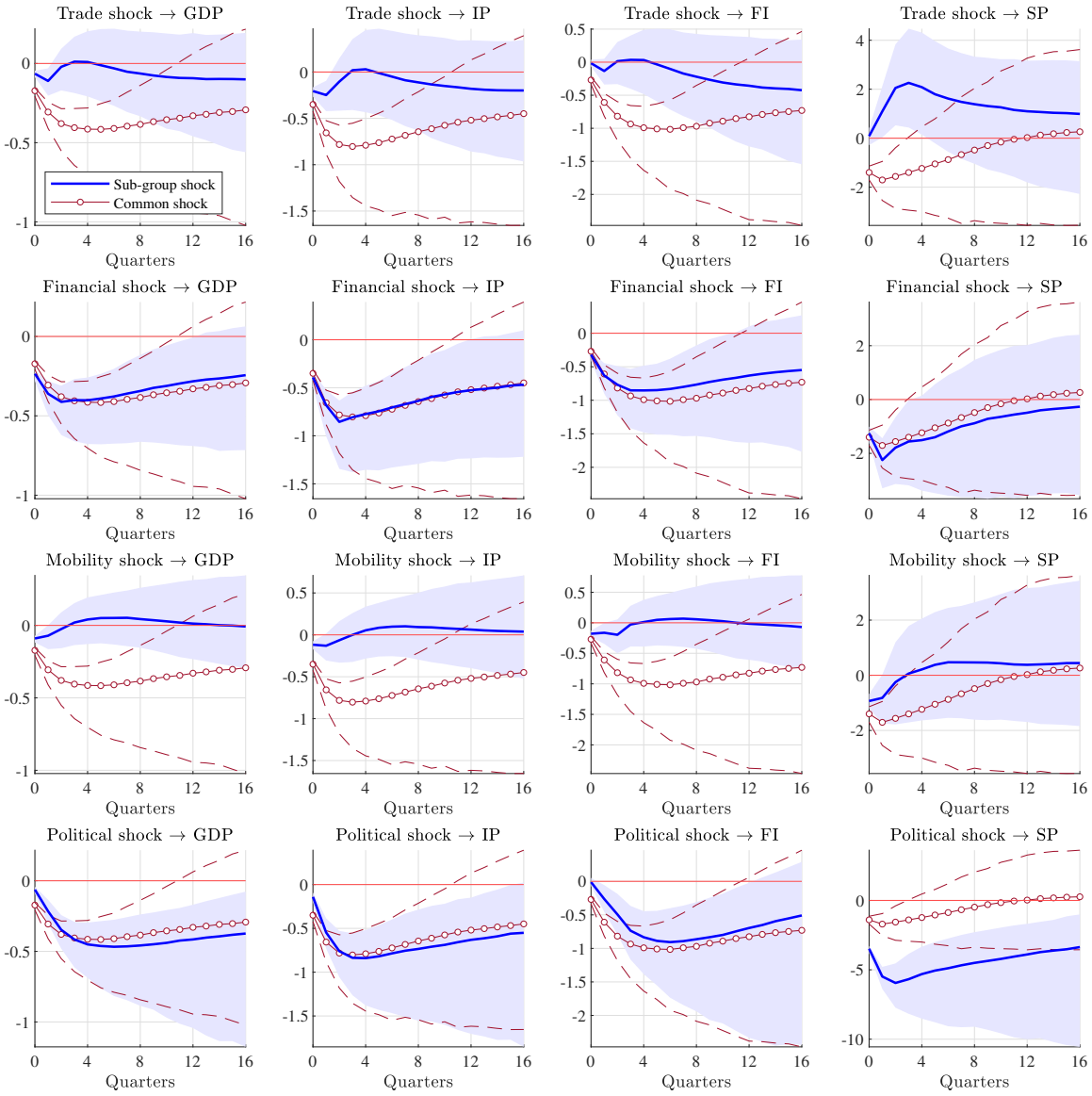

Notes: Sample of AEs and EMs. Percent responses to a one-standard-deviation shock. Shaded areas indicate the 90th percentiles where standard errors are clustered by time. Sub-group shocks are identified as those that have zero impacts on the other sub-group indices while increasing their own sub-group and common index in the 8-quarter horizon. The IRFs to the baseline global fragmentation shock (Cholesky decomposition) are shown in lines with circles as a reference.